Naval Coastal Systems Center

Panama City, Florida 32407-5000

AD-A222 606

CONTRACTOR REPORT
NCSC CR 20C-1-90

MAY 1990

DEVELOPMENT OF MEMBRANE PROCESS FOR CARBON DIOXIDE SEPARATION FROM DIVING ATMOSPHERE

S. A. STERN

K. A. LOKHANDNALA

Dept. of Chemical Engineering and Materials Science
Syracuse University
Syracuse, NY 13244

Prepared for
Naval Coastal Systems Center
Panama City, Florida 32407-5000

ABSTRACT

Computer simulations have shown that membrane separation processes can be used effectively to remove CO_2 from exhaled air in an underwater breathing apparatus. Membrane separation processes are based on the selective permeation of the components of a gas mixture through nonporous polymer membranes.

A permeator module provided with membranes in the form of asymmetric or "composite" hollow fibers is best suited for CO_2 removal from exhaled air. The operation of such a permeator, designed to reduce the CO_2 concentration in exhaled air from about 4 mole-% to 1 mole-%, has been simulated in order to determine its optimum dimensions and membrane area requirement. The exhaled air will flow in such a permeator in an axial direction inside the hollow fibers, while the external surface of the fibers will be in contact with sea water. The fraction of the exhaled air permeating through the hollow fibers (the "permeate") will be enriched in CO_2 which will be dissipated in the sea water.

SUMMARY

Computer simulations have shown that membrane separation processes can be used effectively to remove CO_2 from exhaled air in an underwater breathing apparatus. Membrane separation processes are based on the selective permeation of the components of a gas mixture through nonporous polymer membranes.

A permeator module provided with membranes in the form of asymmetric or "composite" hollow fibers is best suited for CO_2 removal from exhaled air. The operation of such a permeator, designed to reduce the CO_2 concentration in exhaled air from about 4 mole-% to 1 mole-%, has been simulated in order to determine its optimum dimensions and membrane area requirement. The exhaled air will flow in such a permeator in an axial direction inside the hollow fibers, while the external surface of the fibers will be in contact with sea water. The fraction of the exhaled air permeating through the hollow fibers (the "permeate") will be enriched in CO_2, which will be dissipated in the sea water.

Keywords: Membrane Separation Process, Diving, Computerized Simulation, Hollow-fiber Permeator Modules, UBA, Marine Atmospheres

It was assumed that the hollow fiber membranes will be made from either ethyl cellulose or an acrylonitrile/butadiene copolymer, and that their effective thickness will be 1000 Å. For an exhaled air rate of 60 ltr(STP)/min (corresponding to a medium diver work-load), the required membrane area will be only about 14 ft^2 if the membrane is made of ethyl cellulose. Assuming a conservative fiber-packing density of 1000 ft^2/ft^3, this membrane area can be housed in a cylindrical permeator only 1.75" (4.44 cm) in diameter and 9.6" (24.4 cm) long. The dimensions of the hollow fibers will be 0.0275" (0.07 cm) I.D. and 0.0315" (0.08 cm) O.D. The pressure drop in the permeator will be less than 4cm-H_2O.

Hence, hollow-fiber permeator modules will be much more compact and lighter than the soda-lime canisters used at present for CO_2 removal.

TABLE OF CONTENTS

DEVELOPMENT OF A MEMBRANE PROCESS FOR CARBON DIOXIDE SEPARATION FROM DIVING ATMOSPHERES

I. INTRODUCTION

The general objective of this project is to develop a membrane separation process for the removal of CO_2 from exhaled air in an underwater breathing apparatus (UBA). Membrane separation processes are based on the selective permeation of components of a gas mixture through nonporous membranes, which are commonly made of polymeric materials. The process under consideration in this study is required to reduce the CO_2 concentration in exhaled air from 4 mole-% to less than 1 mole-%. The CO_2 removal is to be performed in a permeator module using "asymmetric" hollow-fiber membranes as separation barriers, because a very large membrane area can be packed per unit volume in such modules. A simplified diagram of the CO_2 removal process is shown in Figure 1. The feasibility of the process has been investigated by means of different computer simulations.

The following studies have been performed since the previous progress report was filed:

1. A computer program has been developed to simulate the removal of CO_2 from exhaled air in a hollow-fiber permeator operating under realistic "cross-flow" conditions. In this permeator, exhaled air (the "feed") is taken to flow inside the hollow fibers, whereas the permeated gas emerges from the hollow fibers in a direction perpendicular to the feed flow (see Appendix I). The permeated gas, enriched in CO_2, is dispersed in sea water, which will be in contact with the external surfaces of the hollow fibers. The pressure drop occurring inside the hollow fibers has also been computed.

The simulation described in the previous report assumed flat-sheet

membranes, simplified "perfect-mixing" conditions in the feed and permeate streams, and negligible pressure drop in the permeator.

2. More realiable values of membrane permeability and selectivity to CO_2, O_2 and N_2 were used in the new study. In earlier studies the membrane was assumed to be made from cellulose acetate, and the values of the permeability coefficients for CO_2, O_2, and N_2 in this polymer were taken from the Polymer Handbook (1), a well-known reference text. However, an examination of the literature and discussions with an industrial organization indicated that the selectivity of cellulose acetate toward CO_2 relative to O_2 and N_2 was lower than indicated in the above Handbook. Therefore, membranes made of polymers other than cellulose acetate were considered for CO_2 separation.

3. The effects of diving depth on the membrane area requirement were investigated. The rates of gas permeation of the components of exhaled air depend strongly on this parameter. Depths from 5 to 100 FSW were assumed in the computations. A depth of 10 FSW was taken for the calculations of membrane area requirements and of O_2 loss.

4. The concentrations of CO_2, O_2 and N_2 dissolved in sea water, and their effects on the CO_2 separation process, were taken into consideration in the new process simulations.

The results of this study are discussed below.

II. DESIGN OF PERMEATOR MODULE

A. General Considerations

Excess CO_2 will be removed from the exhaled air in a hollow-fiber permeator module. A diagram of such a permeator is shown in Figure 2. The permeator, as modified for the present application, will consist of a light-weight cylindrical vessel containing a bundle of hollow fiber membranes. Both

ends of the hollow fibers will be "potted" (encased) in tube sheets, or "headers", made of epoxy resin. The section of the cylindrical vessel between the tube sheets will be perforated in order to allow sea water to contact and circulate around the hollow fibers.

Exhaled air (the "feed") will enter one end of the permeator module as shown in Figure 2, and will flow inside the hollow fibers in an axial direction. A fraction of the feed gas will permeate through the walls of the hollow fibers and dissolve in the sea water surrounding the fibers. The permeated gas (or "permeate") will be enriched in CO_2, because the permeability of the hollow fibers to CO_2 will be higher than to the other components of exhaled air, i.e., mainly O_2 and N_2. The unpermeated gas remaining inside the hollow fibers (sometimes called the "retentate") will be depleted in CO_2, the partial pressure of CO_2 decreasing from the inlet to the outlet of the permeator. The permeate can be visualized as flowing in a direction perpendicular to the feed flow, as is shown in Figure 3. This flow pattern is known as "cross-flow."

The amount of CO_2 removed from the exhaled air by selective permeation through the hollow fibers will depend on the following factors (see Appendix II):

1. The composition of the feed (i.e., of the exhaled air).
2. The nature of the polymer from which the hollow fibers are made.
3. The concentration of CO_2 inside and outside the hollow fibers; the difference in these concentrations is the driving force for permeation.
4. The temperature.

B. Description of Hollow-Fiber Membranes

The hollow-fiber membranes will be asymmetric (anisotropic) in a

direction perpendicular to their surfaces. Asymmetric membranes consist of a highly porous substrate which is 3-6 mil (76.2-152.4 μm) thick and is provided with a very thin nonporous surface layer, or "skin", cf. Appendix II. The gas separation process occurs almost entirely in the nonporous skin, whose thickness can be reduced to as little as 2 to 6 x 10^{-3} mil (500 - 1500 Å). The porous substrate serves as a support for the denser skin. Hence, the mechanical properties of an asymmetric membrane are essentially those of its substrate, whereas its gas separation properties (gas selectivity and permeability) are determined by the skin. The presence of pores or pinholes in the dense skin is undesirable because they greatly decrease the membrane selectivity toward different gases.

In some types of asymmetric membranes, the skin is an integral part of the substrate layer, e.g., in cellulosic membranes. In other types of asymmetric membranes, known as "composite membranes", the skin and its substrate are made from different polymers. The gas separation and mechanical properties of such membranes can be optimized separately (see Appendix II).

The use of membranes in the form of asymmetric hollow fibers (Figures 4a and 4b) has two important advantages:

1. The rate of gas permeation through a nonporous membrane is inversely proportional to its effective thickness, as is shown below. Since the effective thickness of an asymmetric membrane is that of its dense skin, which is very thin, the rate of permeation per unit membrane area can be large.

2. The fact that asymmetric membranes can be produced in the form of small-bore hollow fibers makes it possible to pack very large membrane areas in small volumes (3000 to 8000 ft^2/ft^3, depending on the fiber diameter and packing density). Hence, hollow-fiber permeators are very compact.

The dense skin is usually formed on the feed-side of the hollow fibers.

Hence, in the present application the skin will be on the internal surface of the hollow fibers, cf. Figure 4b.

C. Mechanism of Gas Permeation

Gases permeate through nonporous membranes by a "solution-diffusion" mechanism, which has been discussed elsewhere (2,3) and is also described in Appendix II.

The permeation of a gas through a nonporous membrane can be generally described by Fick's laws (2,3). The steady-state rate of gas permeation, Q_s, through a long hollow cylinder, such as a hollow-fiber membrane, is then given by the isothermal expression:

$$Q_s = D \frac{2\pi L(c_2^M - c_1^M)}{\ell n[R_O/R_I]} \qquad (1)$$

where D is the mutual diffusion coefficient for the gas/membrane system of interest; L is the length of the hollow fiber; R_O and R_I are the outer and inner radii of the hollow fiber, respectively; c_2^M and c_1^M ($<c_2^M$) are the penetrant gas concentrations of the outer and inner surfaces of the hollow fiber, respectively. D is assumed here to be independent of the penetrant concentration, and superscript M refers to the hollow-fiber membrane.

When the hollow fiber is asymmetric, as will be the case in the present application, the radii of interest are those of the dense skin. Since this skin is very thin, i.e., $R_O/R_I \approx 1$, the denominator in eqn. (1) can be expanded in series:

$$\ell n(R_O/R_I) = \left[(R_O/R_I)-1\right] - \ldots = \frac{\delta}{R_I} , \qquad (2)$$

where $\delta (=R_O - R_I)$ is the thickness of the dense skin. Equations (1) and (2) then yield:

$$Q_s = D \frac{2\pi R_I L}{\delta} (c_2^M - c_1^M) = \frac{DA}{\delta} (c_2^M - c_1^M) \quad . \qquad (3)$$

where $A(=2\pi R_I L)$ is the inner surface area of the dense skin.

In the present application the penetrant gas will be exhaled air (the feed) which will flow inside the hollow fibers in an axial direction. As mentioned earlier, the dense skin will be formed on the inner surface of the hollow fibers. Let the local concentration of any component i of exhaled air (O_2, N_2, or CO_2) dissolved in the skin at the feed-side interface be denoted $c_{F,i}^M$, cf. Figure 5. Let also the local partial pressure of component i in the exhaled air be $p_A \cdot x_i$, where p_A is the total local pressure of the exhaled air inside the hollow fibers, and x_i is the local mole-fraction of component i in the exhaled air. If solution equilibrium is established between component i in the exhaled air and in solution in the dense skin at the feed/skin interface, one can write the isothermal relation:

$$c_{F,i}^M = S_i (p_A \cdot x_i), \qquad (4)$$

where S_i is a solubility coefficient which depends only on the nature of component i and the dense skin, and on temperature.

The outer surface of the hollow-fiber membranes will be in contact with sea water, which will also impregnate the porous substrate of the hollow fibers. Consequently, the outer surface of the dense skin will also be in contact with sea water. It should be noted that this surface is also the interface between the skin and its porous substrate. Let the concentrations of component i dissolved in the dense skin and in sea water at the skin/sea-water interface be denoted $c_{P,i}^M$ and $c_{P,i}^{SW}$, respectively. One can then write the equilibrium relation, cf. Figure 5:

$$c_{P,i}^M = K_i c_{P,i}^{SW} \quad . \qquad (5)$$

where K_i is a partition coefficient. K_i will also depend on the nature of component i and of the skin, and on temperature. Equations (3)-(5) then yield:

$$Q_{s,i} = \frac{2\pi R_1 L D_i (S_i p_A x_i - K_i c_{P,i}^{SW})}{\delta} = \frac{2\pi R_1 L D_i}{\delta} (S_i p_A x_i - K_i c_{P,i}^{SW}) \qquad (6)$$

The concentration $c_{P,i}^{SW}$ cannot be measured, particularly since the dense skin of an asymmetric membrane may not have a distinct interface with its porous substrate. Therefore, it will be assumed that $c_{P,i}^{SW}$ will be identical with the concentration of component i in bulk sea water, cf. Figure 5. Hence, $c_{P,i}^{SW}$ will depend on the solubility of component i in sea water, on its partial pressure in the atmosphere, on the temperature of sea water, on the salinity of the water. and on depth. Therefore, it is possible to assume the relation, cf. Figure 5:

$$c_{P,i}^{SW} = H_i (p_{atm} \cdot y_{i,atm}) \qquad (7)$$

where p_{atm} is the atmospheric pressure; $y_{i,atm}$ is the mole-fraction of component i in the atmosphere, and H_i is a suitable solubility coefficient. The solubility of i (O_2, N_2, CO_2) in sea water probably will be within Henry's law limit. Equations (6) and (7) then yield

$$Q_{S,i} = P_i \frac{2\pi R_1 L}{\delta} (p_A x_i - K_i' p_{atm} y_{i,atm}), \qquad (8)$$

where $P_i (= D_i S_i)$ is a permeability coefficient. and $K_i' = H_i K_i / S_i$.

Let component i be CO_2. It is evident that the rate of CO_2 permeation through hollow fiber membranes will be large if:

a) D_{CO_2} and S_{CO_2}, and hence P_{CO_2}, are large.

b) H_{CO_2} and K_{CO_2}, and hence K'_{CO_2}, are small.

c) The dense skin is very thin, i.e., δ is very small.

Moreover, the skin substrate must be highly porous in order to permit

easy circulation of the sea water to and from the permeate-side of the dense skin. This could best be achieved with "composite" hollow fibers.

III. SELECTION OF MEMBRANE MATERIAL

In a previous simulation of a membrane process for the removal of CO_2 from exhaled air it was assumed that the membranes will be made from cellulose acetate (4). The Polymer Handbook (1) cites the following values of the permeability coefficients for CO_2, O_2, and N_2 in cellulose acetate at 30°C:

$$\bar{P}_{CO_2} = 22.7 \times 10^{-10} \text{ cm}^3\text{(STP)}\cdot\text{cm}/(\text{s}\cdot\text{cm}^2\cdot\text{cmHg})$$

$$\bar{P}_{O_2} = 0.78 \times 10^{-10} \quad " \quad " \quad " \quad "$$

$$\bar{P}_{N_2} = 0.28 \times 10^{-10} \quad " \quad " \quad " \quad "$$

The selectivity of cellulose acetate toward CO_2 relative to O_2 and N_2, respectively, is then given by the respective ideal separation factors:

$$\alpha^*(CO_2/O_2) \equiv \bar{P}_{CO_2}/\bar{P}_{O_2} = 29.1$$

$$\alpha^*(CO_2/N_2) \equiv \bar{P}_{CO_2}/\bar{P}_{N_2} = 81.1$$

However, an examination of the literature has indicated that the above selectivities are too high because the permeability coefficient for CO_2 was not obtained with the same type of cellulose acetate as the permeability coefficients for O_2 and N_2 (5). More recent publications indicate that $\alpha^*(CO_2/O_2) = 7.3$ and $\alpha^*(CO_2/N_2) = 21.7$ for an unspecified type of cellulose acetate at 25°C. These lower selectivities were confirmed by an industrial manufacturer of cellulose acetate membranes.

The literature also shows that the following polymer membranes have selectivities toward CO_2, relative to O_2 and N_2, comparable to those of cellulose acetate, but have much higher gas permeabilities:

Polymer	Permeability Coefficient, $\bar{P} \times 10^{10}$ [$cm^3(STP) \cdot cm/(s \cdot cm^2 \cdot cmHg)$]		
	CO_2	O_2	N_2
Ethyl cellulose (ethoxy 49.5%) (6)	113.0	14.7	4.43
Acrylonitrile/butadiene block copolymer (7)	30.9	3.84	1.1

The above data are for a temperature of 25°C. The corresponding selectivities are:

Polymer	$\alpha^*(CO_2/O_2)$	$\alpha^*(CO_2/N_2)$
Ethyl cellulose (ethoxy 49.5%)	7.7	25.5
Acrylonitrile/butadiene block copolymer	8.0	28.1

The above two polymers have been considered in the following calculations as materials for the preparation of composite hollow fibers for CO_2 removal from exhaled air. It should be noted that ethyl cellulose is a glassy polymer at ambient temperature, whereas the A/B block copolymer is in the "rubbery" state. Therefore, these two materials have significantly different mechanical properties.

IV. PROCESS SIMULATIONS

A. Objectives

The objectives of the process simulations were as follows:

1. To determine the membrane area required to reduce the CO_2 content in exhaled air from about 4 mole-% (more exactly 3.93 mole-%) to 1 mole-% in a permeator module with asymmetric or "composite" hollow fiber membranes.

2. To determine the dimensions of the permeator module required to perform the above separation.

3. To determine the loss of oxygen in the permeator module.

4. To determine the inner diameter of the hollow fibers necessary to reduce the axial pressure drop across the permeator module to required specifications (4 cm-H_2O medium load) (8).

B. Basis of Calculations

The composition of exhaled air at the inlet of the permeator module, i.e, in the feed, was taken to be as follows (8):

Component	Mole-fraction, y_i
CO_2	0.0393
O_2	0.1675
N_2	0.7763
H_2O vapor	0.0177
	1.0000

The feed is assumed to be saturated with water vapor at 25°C. Since the permeate-side of the hollow fibers will be in contact with sea water, the activity of H_2O will be approximately the same on the two sides of the hollow fibers. Consequently, no significant transfer of H_2O is expected to take place from the permeate-side to the feed-side of the hollow fibers or vice versa.

The concentrations of CO_2, O_2, and N_2 in sea water at a depth of 10 FSW were calculated to be as follows (in terms of mole-fractions and partial pressures):

Component	Mole-fraction	Partial Pressure (bars)
CO_2	5.85×10^{-4}	7.78×10^{-4}
O_2	2.28×10^{-5}	3.04×10^{-5}
N_2	1.025×10^{-5}	1.36×10^{-5}

It is seen that the concentration of the above gases in sea water is negligibly small compared to that in exhaled air.

It was assumed that the CO_2 concentration in the exhaled air at the

outlet of the permeator module is reduced to 1 mole-%. The air is then recycled to the diver. The flow rate of exhaled air into the permeator was taken to be 1,000 cm^3(STP)/s, and the effective membrane thickness, i.e., the thickness of the dense skin, was taken to be 1000 Å.

V. DISCUSSION OF RESULTS

A. Process Simulations

The results of the process simulations are presented graphically in Figures 6 to 18. The results obtained for ethyl cellulose membranes are presented first in Figures 6 to 12, which are discussed below.

Figure 6 shows the membrane area required to reduce the CO_2 content of exhaled air from about $x^o_{CO_2}$ = 0.04, or 4 mole-%, to lower values; $x^o_{CO_2}$ is the mole-fraction of CO_2 at the permeator outlet. The membrane area is seen to increase sharply as the CO_2 concentration remaining in the exhaled air is decreased. However, due to the high rate of CO_2 permeation through asymmetric hollow fibers made of ethyl cellulose, only about 14 ft^2 will be required to reduce the CO_2 concentration to $x^o_{CO_2}$ = 0.01, or 1 mole-%. This membrane area can be packed, as will be shown below, in a very small permeator module.

Oxygen and nitrogen will permeate through the hollow fibers together with CO_2, albeit at a much slower rate, cf. Section III. Consequently, some of the O_2 in the exhaled air will be lost in the permeate. Figure 7 shows the %-O_2 lost as the concentration of CO_2 in the exhaled air is decreased. For example, when the CO_2 concentration at the permeator outlet is reduced to $x^o_{CO_2}$ = 0.02, or 2 mole-%, the O_2 loss will be about 8.2%. The O_2 concentration in the exhaled air will then be reduced from $x^I_{O_2}$ = 0.1675 at the permeator inlet to $x^o_{O_2}$ = 0.1542 at the outlet. When the CO_2 content is reduced to $x^o_{CO_2}$ = 0.01, or 1 mole-%, about 17% of O_2 will be lost. This loss will have to be

compensated with stored oxygen. The loss of oxygen could be reduced by using hollow-fiber membranes made from polymers which exhibit a higher selectivity for CO_2 relative to O_2, as is shown in a following section.

Figure 8 shows the concentration of CO_2 in the exhaled air at the permeator outlet ($x^o_{CO_2}$) as a function of the "stage cut", i.e., the fraction of the exhaled air (feed) permeating through the hollow fibers. It is seen that a stage cut of about 0.10 is required to reduce the CO_2 concentration to $x^o_{CO_2} = 0.01$.

Figures 9, 10, and 11 show the concentrations of O_2, N_2, and H_2O vapor, respectively, at the permeator outlet as a function of stage cut. It is seen that the concentrations of N_2 and H_2O vapor increase from the inlet to the outlet of the permeator, whereas the concentrations of CO_2 and O_2 decrease.

Figures 12 to 17 present similar data for hollow fibers made from the Acrylonitrile/Butadiene Block copolymer and can be interpreted in a similar way.

B. Pressure Drop Calculations

The pressure drop inside hollow fibers was calculated from eqn. (I-26) in Appendix I. In order to keep the pressure drop below a required value of 4 cm-H_2O as well as to reduce the CO_2 content in exhaled air to 1 mole-%, the dimensions of the hollow fibers will have to be as follows:

Parameters	Hollow Fibers	
	Ethyl Cellulose	A/B Block Copolymer
I.D.	0.0275"(0.07cm)	0.0236"(0.06cm)
O.D.	0.0315"(0.08cm)	0.0315"(0.08cm)
Length	0.80 ft(24.38cm)	0.80 ft(24.38cm)
No. of Hollow Fibers	2,087	8,932

C. Dimensions of Permeator Module

On the basis of the above data, and assuming conservatively a low fiber-packing density of 1,000 ft^2/ft^3, cylindrical permeator modules for CO_2 removal from exhaled air will have the following dimensions.

Ethyl cellulose: Length: 9.6" (24.384 cm), O.D. = 1.75" (4.44 cm)

A/B Block Copolymer: Length: 9.6" (24.384 cm), O.D. = 3.35" (8.51 cm)

Hence, if the assumptions made in the calculations are confirmed by experiment, the permeator module will be both compact and light in weight.

VI. CONCLUSIONS AND PERSPECTIVE

The present study indicates that it is possible to build an efficient permeator module for the removal of CO_2 from exhaled air in an underwater breathing apparatus. If the assumptions made in the computer simulations are validated by experiment, the permeator module will be much more compact and much lighter than the soda-lime canisters used at present for CO_2 removal.

The use of soda-lime canisters limits the time a diver can spend underwater to a few hours. By contrast, permeator modules are inexhaustible, but are subject to some O_2 loss in the permeate. This loss must be compensated with fresh O_2, which increases somewhat the volume of O_2 to be carried by the diver. The magnitude of this loss is illustrated in Figure 7 for ethyl cellulose membranes and in Figure 13 for membranes made from A/B block copolymers.

The oxygen loss in the permeate can be greatly reduced by the use of membranes which exhibit a higher selectivity to CO_2 relative to O_2 than the membranes considered in the present study. This is evident from Figure 18, which shows the decrease in O_2 loss with increasing CO_2/O_2 selectivity at a constant permeability. It is seen that an increase in selectivity from

$\alpha^*(CO_2/O_2) \simeq 7$ (as used in this study) to $\alpha^*(CO_2/O_2) = 30$ would reduce the O_2 loss to less than 20% of that reported in the previous section.

More highly selective membranes of the "facilitated transport" type (cf. Appendix II) are already available. For example, Tajar and Miller (9) have obtained a value of $\alpha^*(CO_2/O_2) = 30.4$ at 30°C and 100% relative humidity with a 4-component membrane system consisting of polyethylenimine-polyvinylbutyral-epoxy-water. More recently, Meldon, Paboojian, and Ranjagam (10) have reported that a composite membrane consisting of polyethylene glycol/alkanolamine mixtures immobilized in microporous polypropylene had a selectivity $\alpha^*(CO_2/O_2) = 40$ at 25°C. In an early study of facilitated transport, Ward and Robb (11) developed a membrane with $\alpha^*(CO_2/O_2) = \underline{4100}$ and a very high permeability to CO_2. The use of such membranes in the present application has not been studied. The facilitated transport membranes described in the literature are relatively thick, but methods of decreasing their effective thickness are being investigated.

Last, but not least, the removal of CO_2 from exhaled air by means of a permeator module is much safer than by using soda-lime canisters, because no chemical reaction takes place in the former device.

REFERENCES

1. "Polymer Handbook", J. Brandrup and E. H. Immergut, Eds., J. Wiley & Sons, New York, 1975, 2nd Ed., p. III-239.

2. S. A. Stern and H. L. Frisch, Ann. Revs. Mater. Sci., 11, 523 (1981).

3. H. L. Frisch and S. A. Stern, Crit. Revs. Solid State and Mat. Sci., 11(2), 123 (1983), CRC Press, Boca Raton, FL.

4. S. A. Stern and H. R. Acharya, "Development of a Membrane Process for Carbon Dioxide Separation from Diving Atmospheres", Progress Report, Dept. of Chemical Engineering and Materials Science, Syracuse University, Syracuse, NY, December 1988.

5. R. Waack, N. H. Alex, H. L. Frisch, V. Stannett, and M. Szware, Ind. Eng. Chem., 47, 2524 (1955).

6. S.-T. Hwang, C. K. Choi, and K. Kammermeyer, Separation Sci., 9(6), 461 (1974).

7. W. J. Koros and R. T. Chern, Chapt. 20 in "Handbook of Separation Process Technology", R. W. Rousseau, Ed., J. Wiley & Sons, New York, 1987, p. 897.

8. J. R. Middleton and E. D. Thalmann, Navy Experimental Diving Unit (NEDU) Report #3-81, "Standardized NEDU Unmanned Test Procedures and Performance Goals", July 1981, AD# A105609, Dept. of the Navy, NEDU, Panama City, FL, 32407.

9. J. G. Tajar and J. Miller, Paper 7b, Spring 1971 National Meeting of American Institute of Chemical Engineers, Houston, TX, February 28 - March 4, 1971.

10. J. Meldon, A. Paboojian, and G. Rajangam, Paper 42c, Symposium on Industrial Membrane Processes, Spring 1985 National Meeting of the American Institute of Chemical Engineers, Houston, TX, March 24-28, 1985.

11. W. J. Ward, III, and W. L. Robb, Science, 156, 1481 (1967).

12. W. L. McCabe, and J. C. Smith, "Unit Operations in Chemical Engineering", McGraw-Hill, New York, 1976, p. 89.

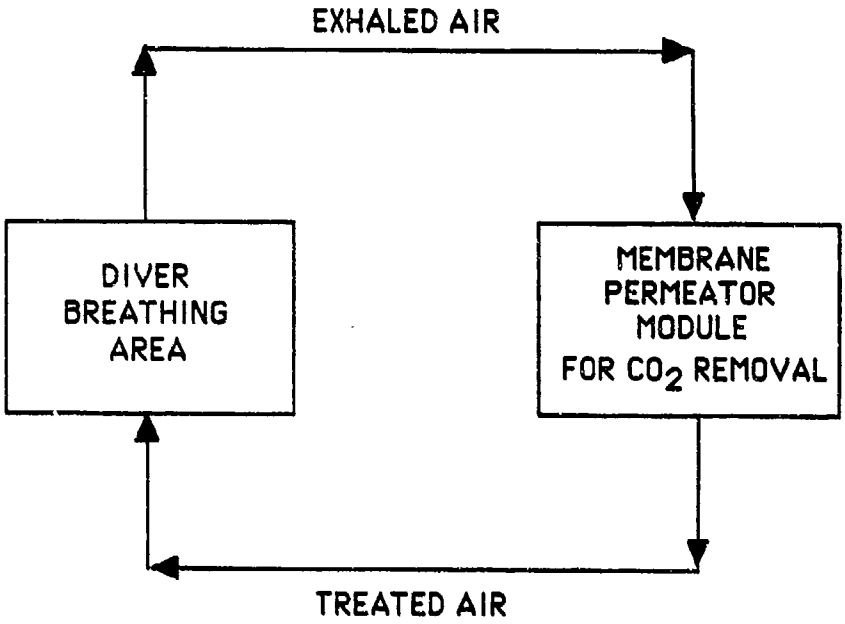

Figure 1: Flow diagram of membrane process of CO_2 removal from exhaled air in an underwater breathing apparatus

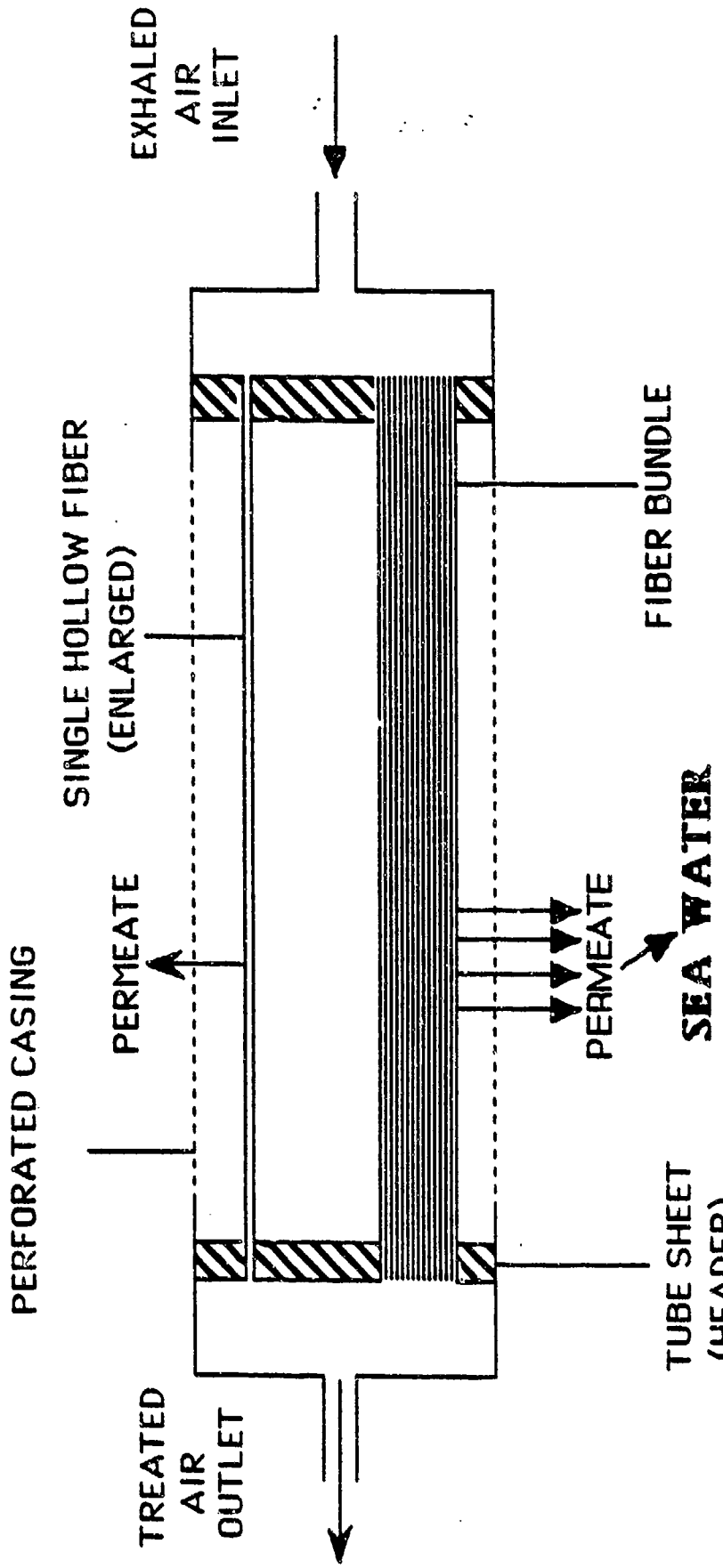

Figure 2: Diagram of permeator module with hollow-fiber membranes

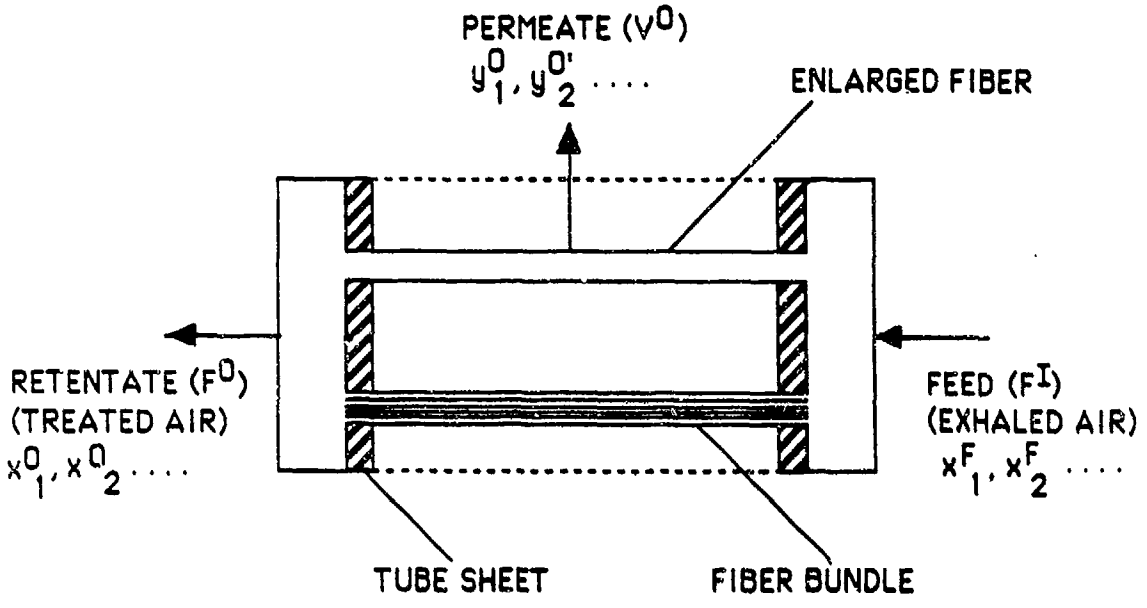

Figure 3: Diagram of permeator module showing the feed, permeate and retentate gas streams. The feed is exhaled air.

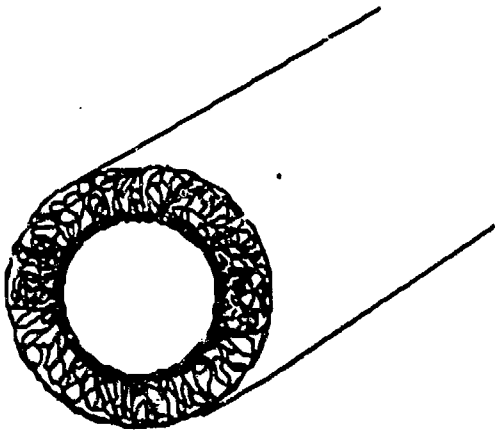

Figure 4a: Cross-section of an asymmetric hollow fiber

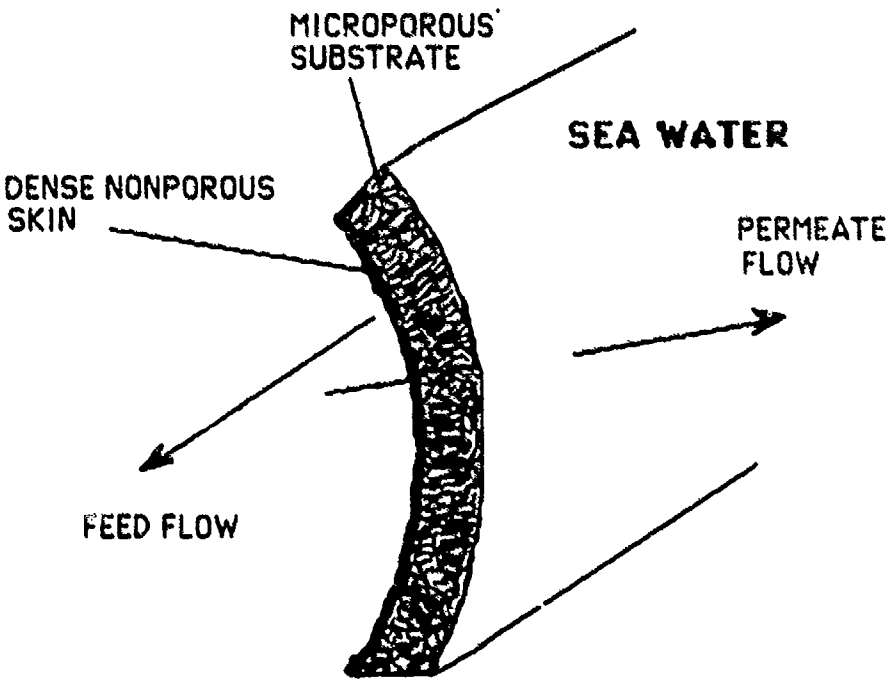

Figure 4b: Enlarged section of a single asymmetric hollow fiber showing the dense skin and porous substrate

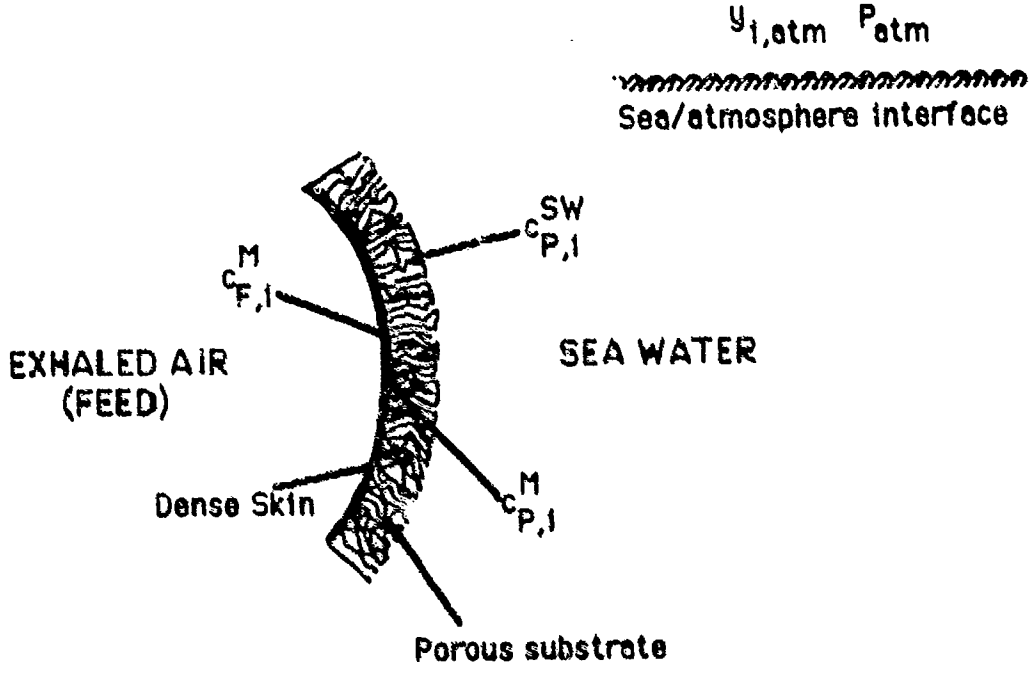

Figure 5: Enlarged section of a hollow fiber showing the concentrations of feed and permeate components within and outside the fiber

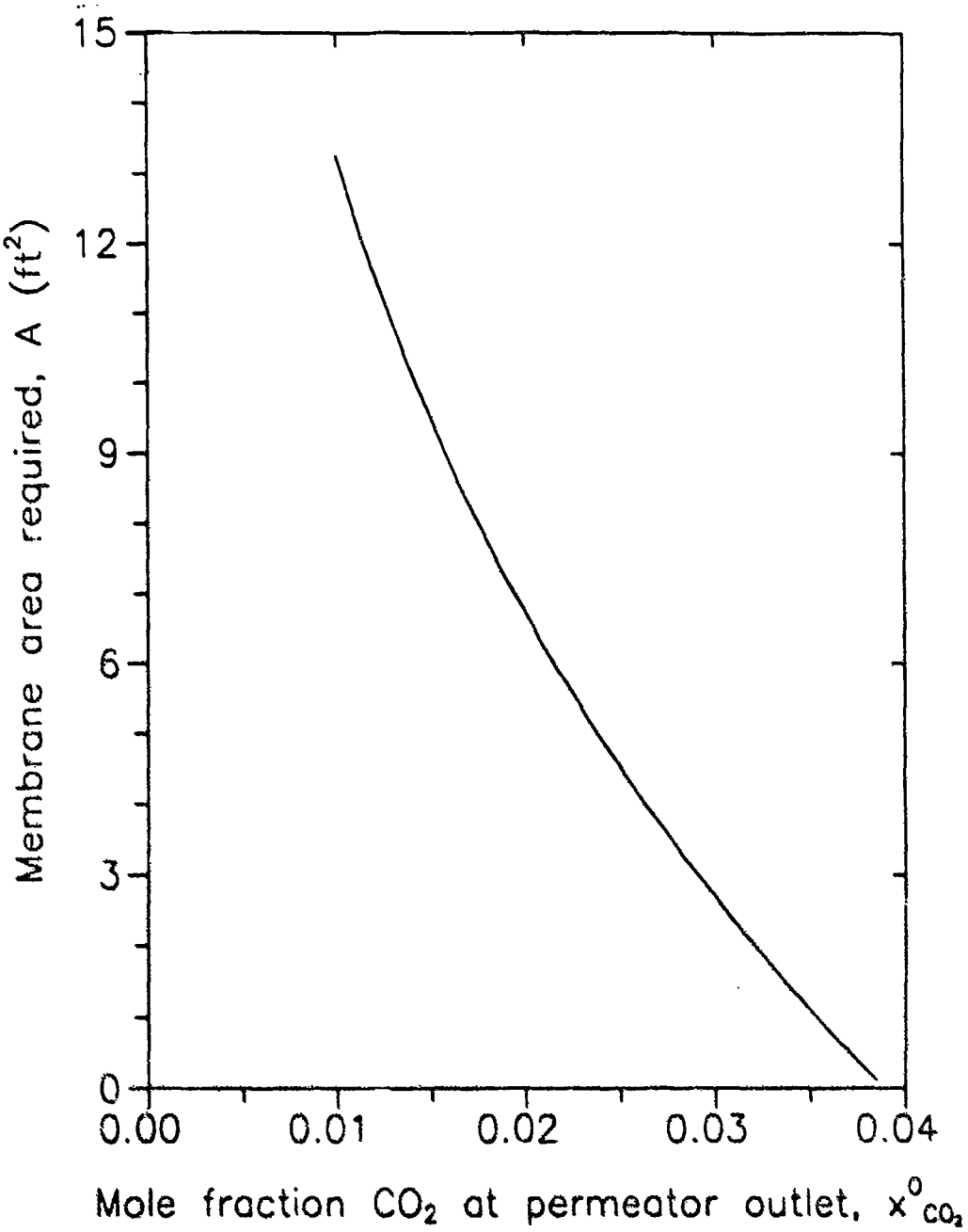

Figure 6: Membrane area required as a function of carbon dioxide concentration at permeator outlet. Membrane material - ethyl cellulose.

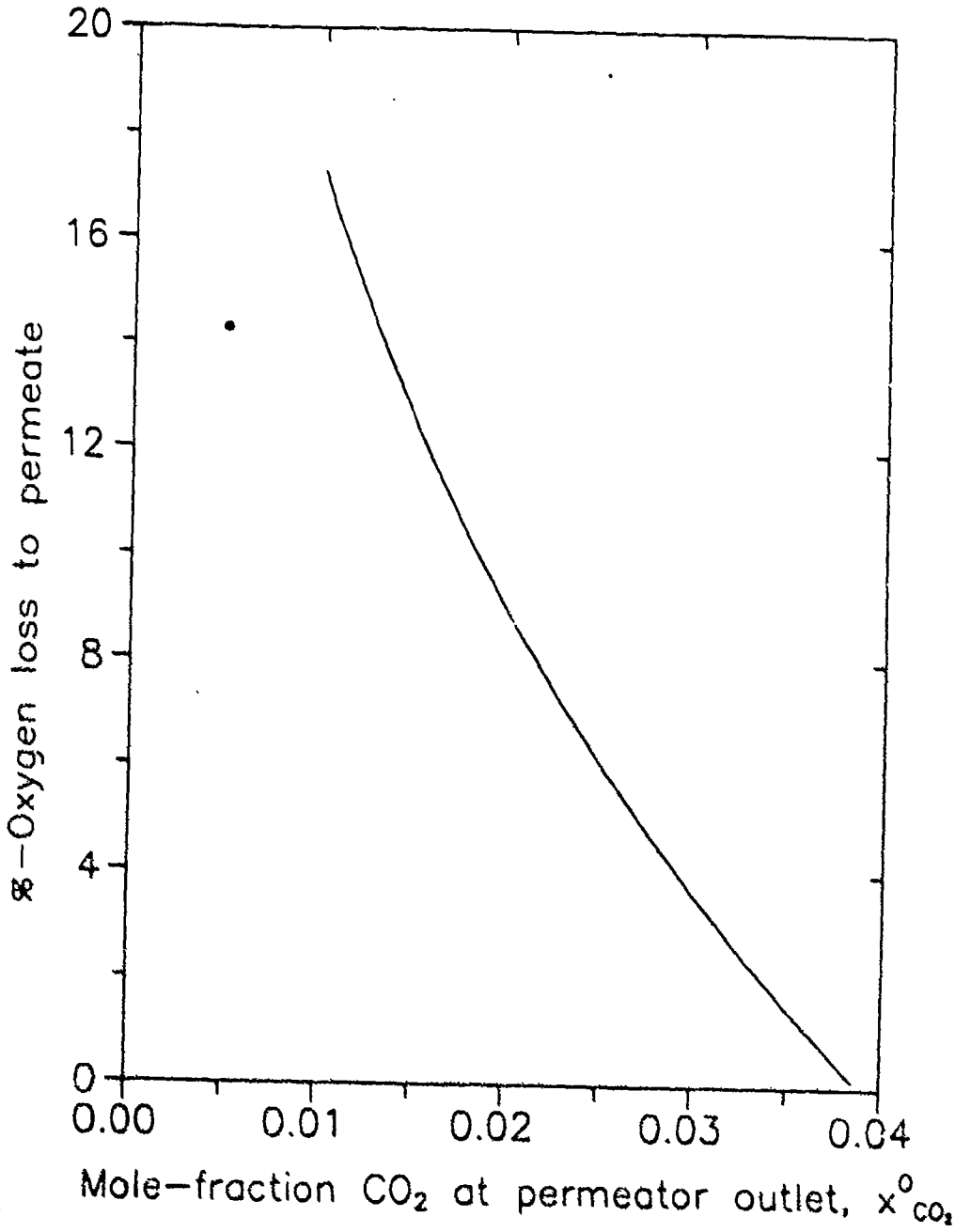

Figure 7. Percent oxygen loss in permeate as a function of carbon dioxide removed from exhaled air. Membrane material - ethyl cellulose.

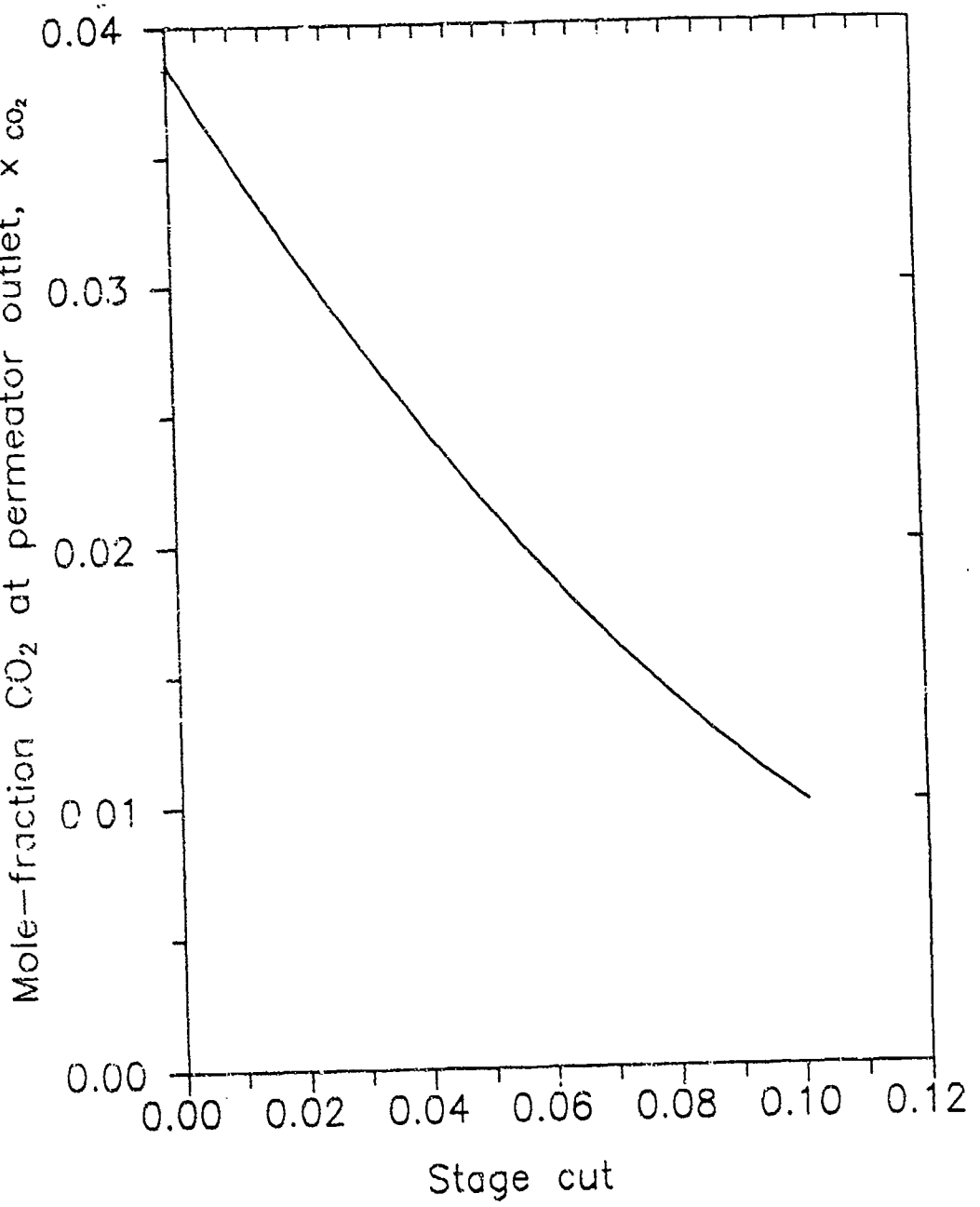

Figure 8: Carbon dioxide concentration in exhaled air at permeator outlet as a function of stage cut. Membrane material - ethyl cellulose.

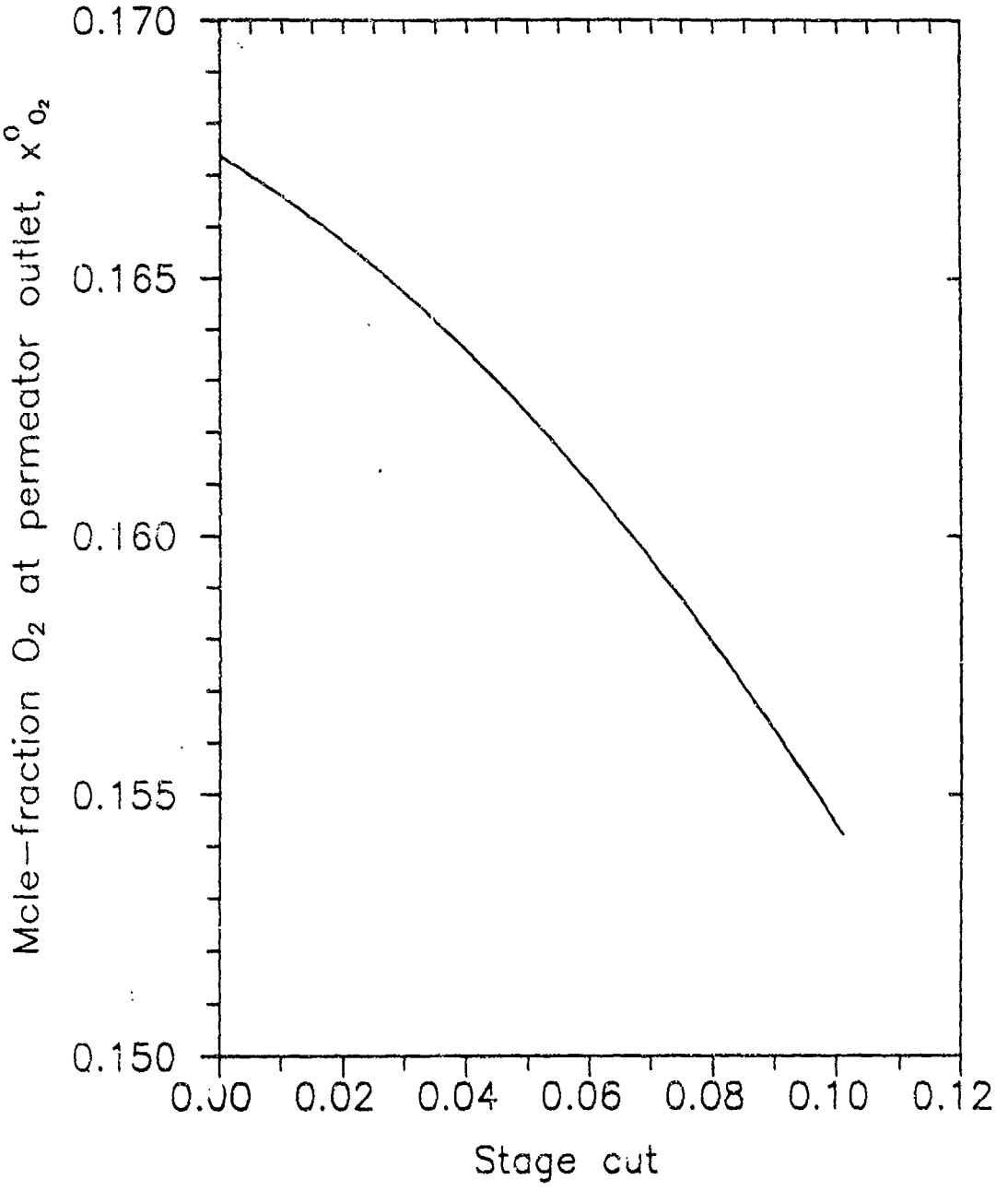

Figure 9: Oxygen concentration in exhaled air at permeator outlet as a function of stage cut. Membrane material - ethyl cellulose.

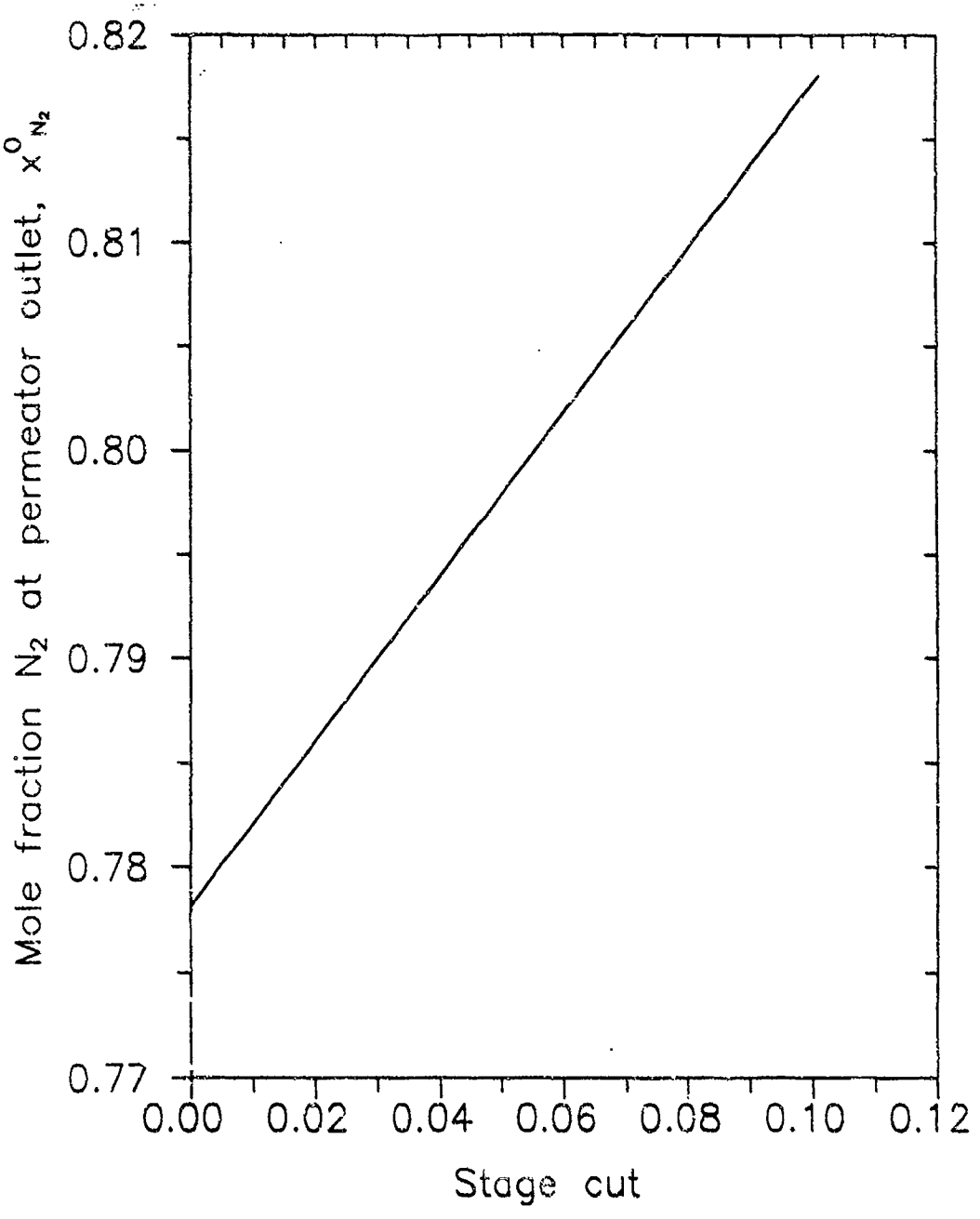

Figure 10: Nitrogen concentration in exhaled air at permeator outlet as a function of stage cut. Membrane material - ethyl cellulose.

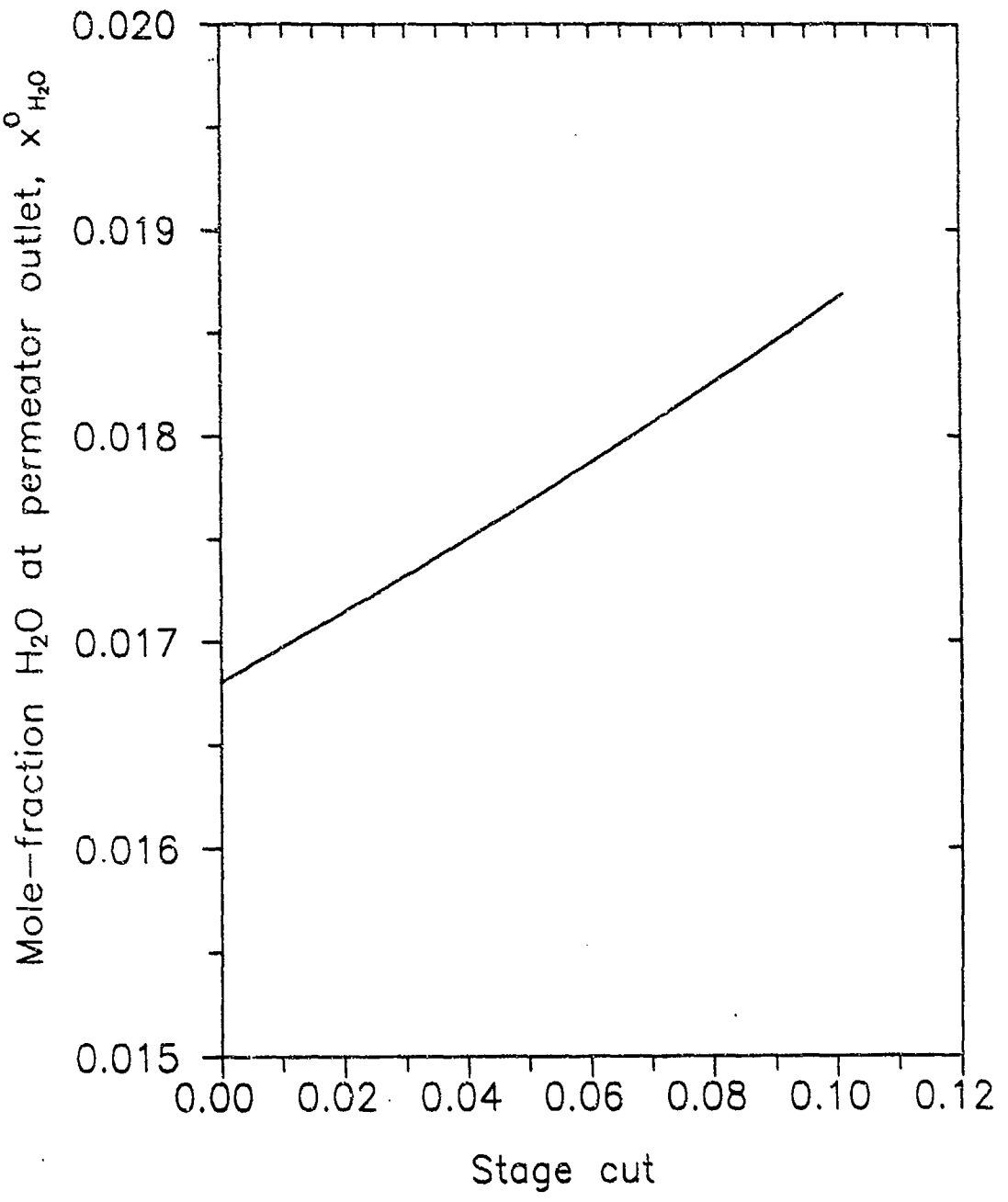

Figure 11: Water vapor concentration in exhaled air at permeator outlet as a function of stage cut. Membrane material - ethyl cellulose.

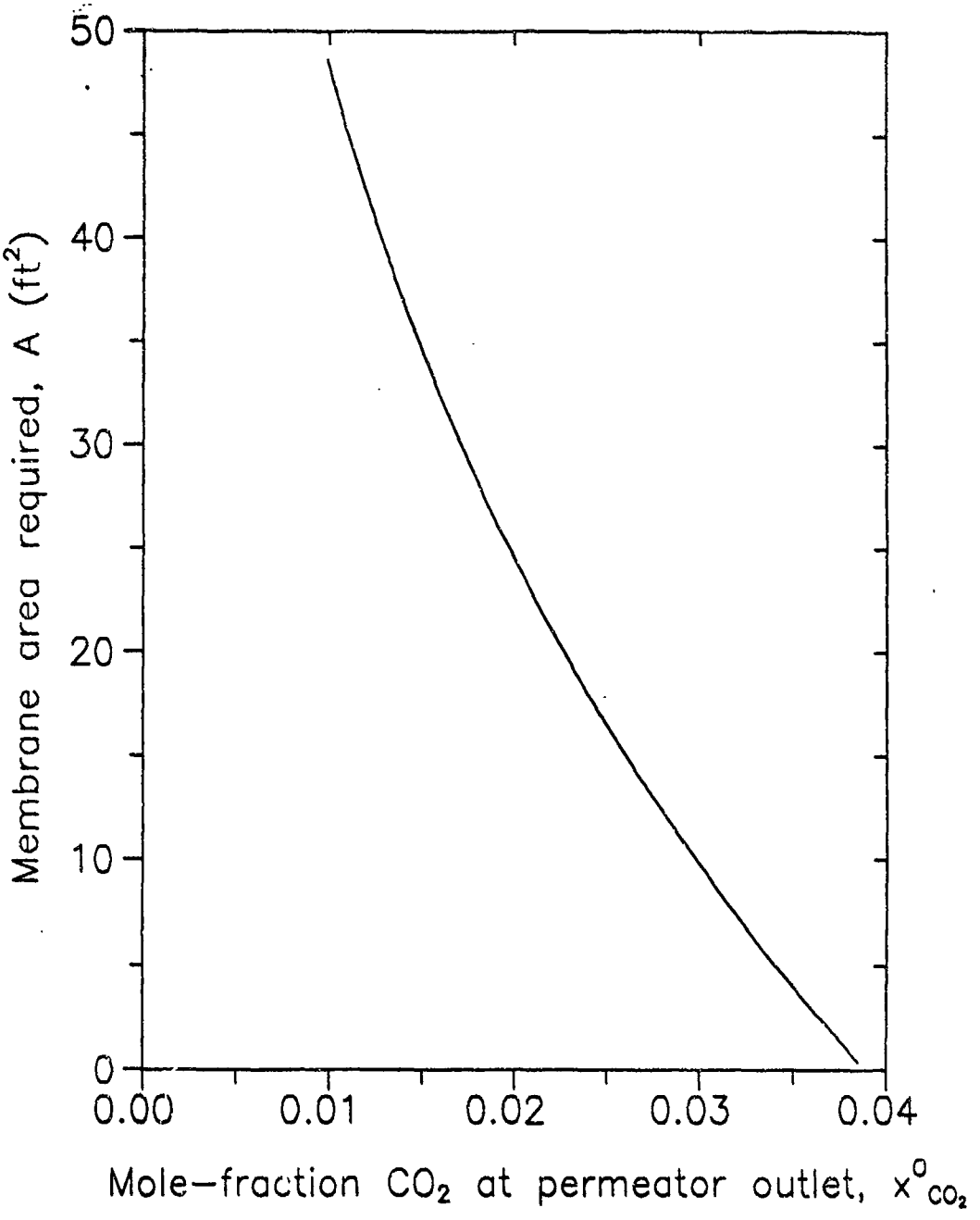

Figure 12: Membrane area required as a function of carbon dioxide concentration at permeator outlet. Membrane material - Acrylonitrile/butadiene copolymer

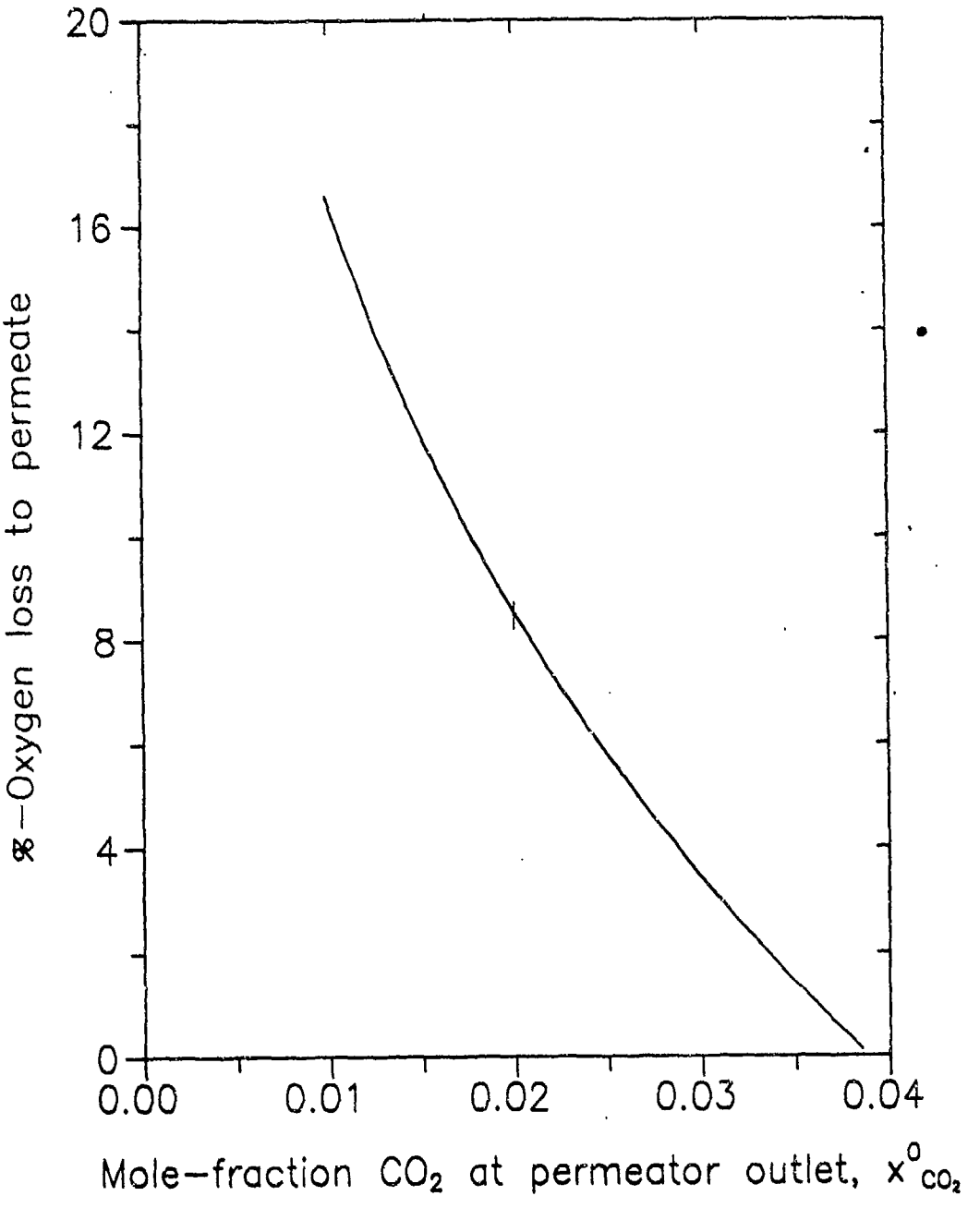

Figure 13: Percent oxygen loss in permeate as a function of carbon dioxide removed from exhaled air. Membrane material - Acrylonitrile/butadiene copolymer.

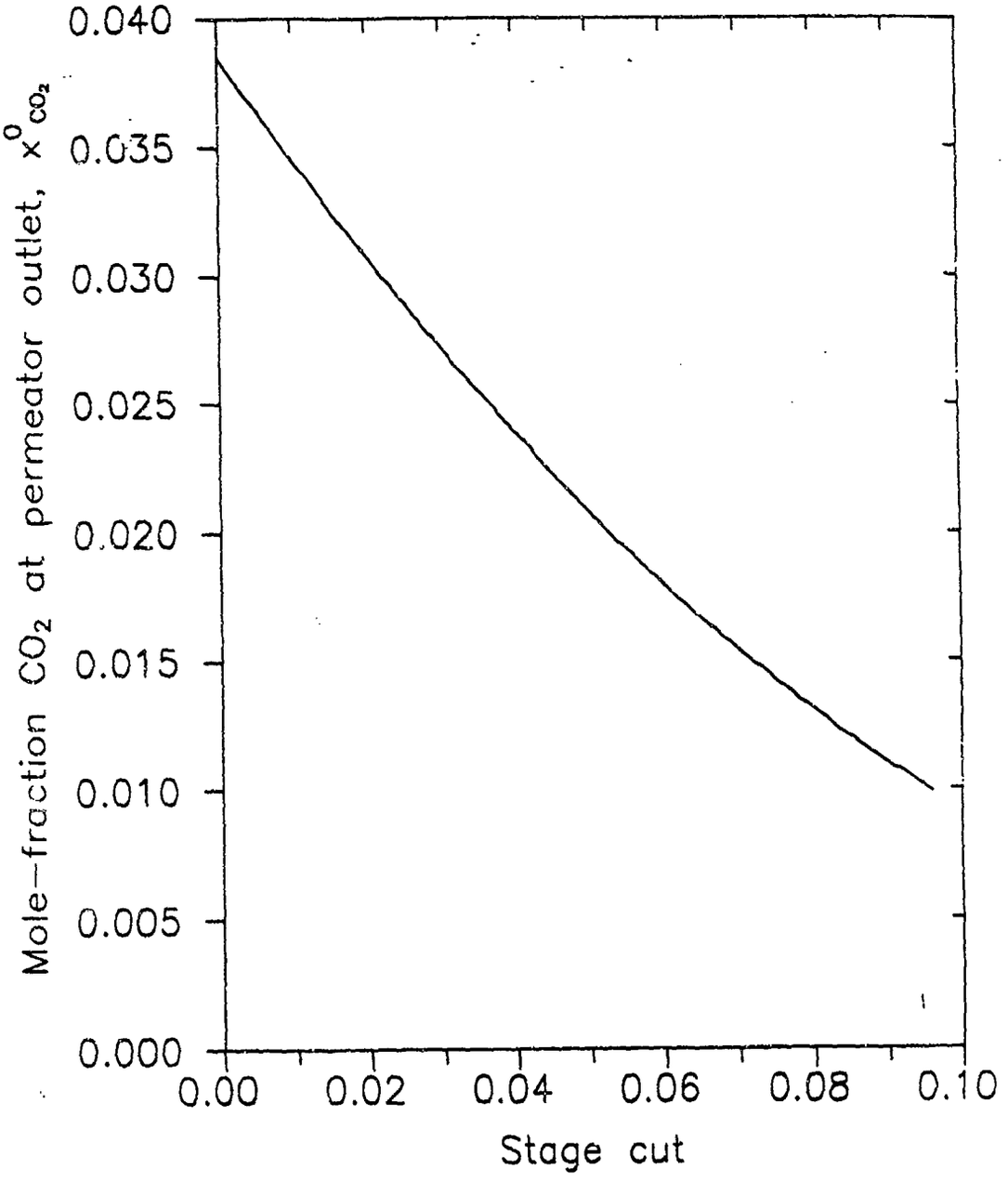

Figure 14: Carbon dioxide concentration in exhaled air at permeator outlet as a function of stage cut. Membrane material - Acrylonitrile/butadiene copolymer.

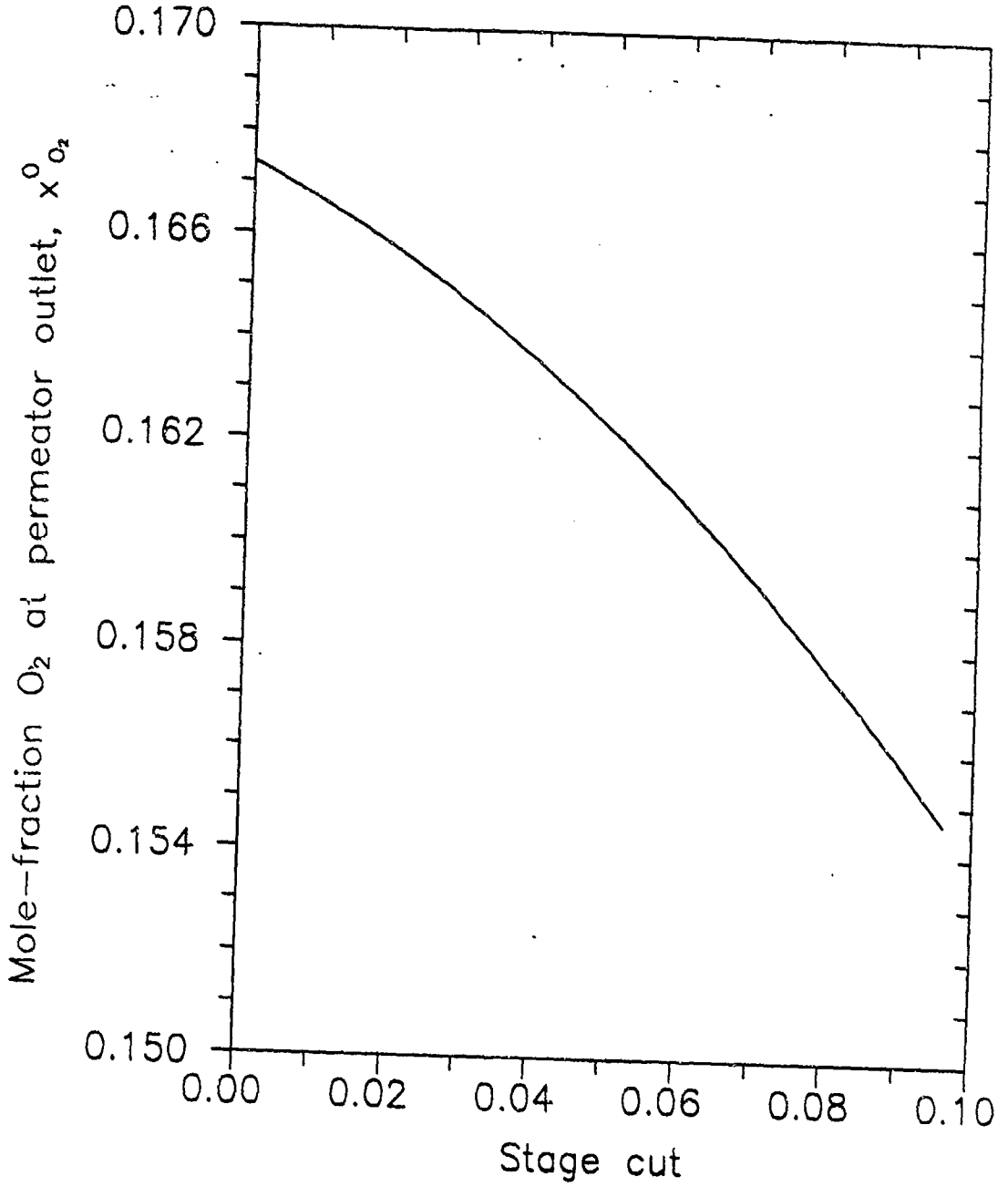

Figure 15: Oxygen concentration in exhaled air at permeator outlet as a function of stage cut. Membrane material - Acrylonitrile/butadiene copolymer.

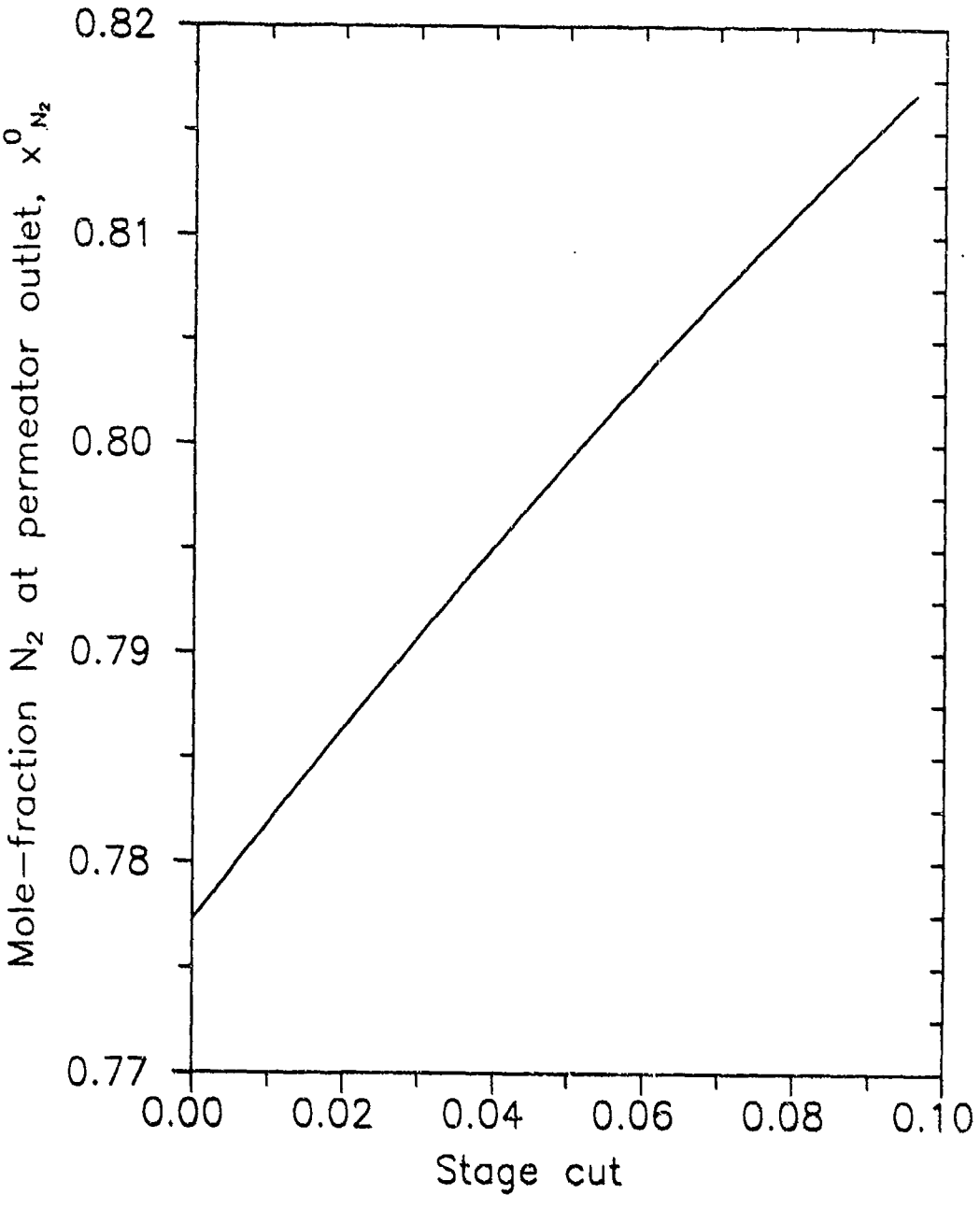

Figure 16: Nitrogen concentration in exhaled air at permeator outlet as a function of stage cut. Membrane material - Acrylonitrile/butadiene copolymer.

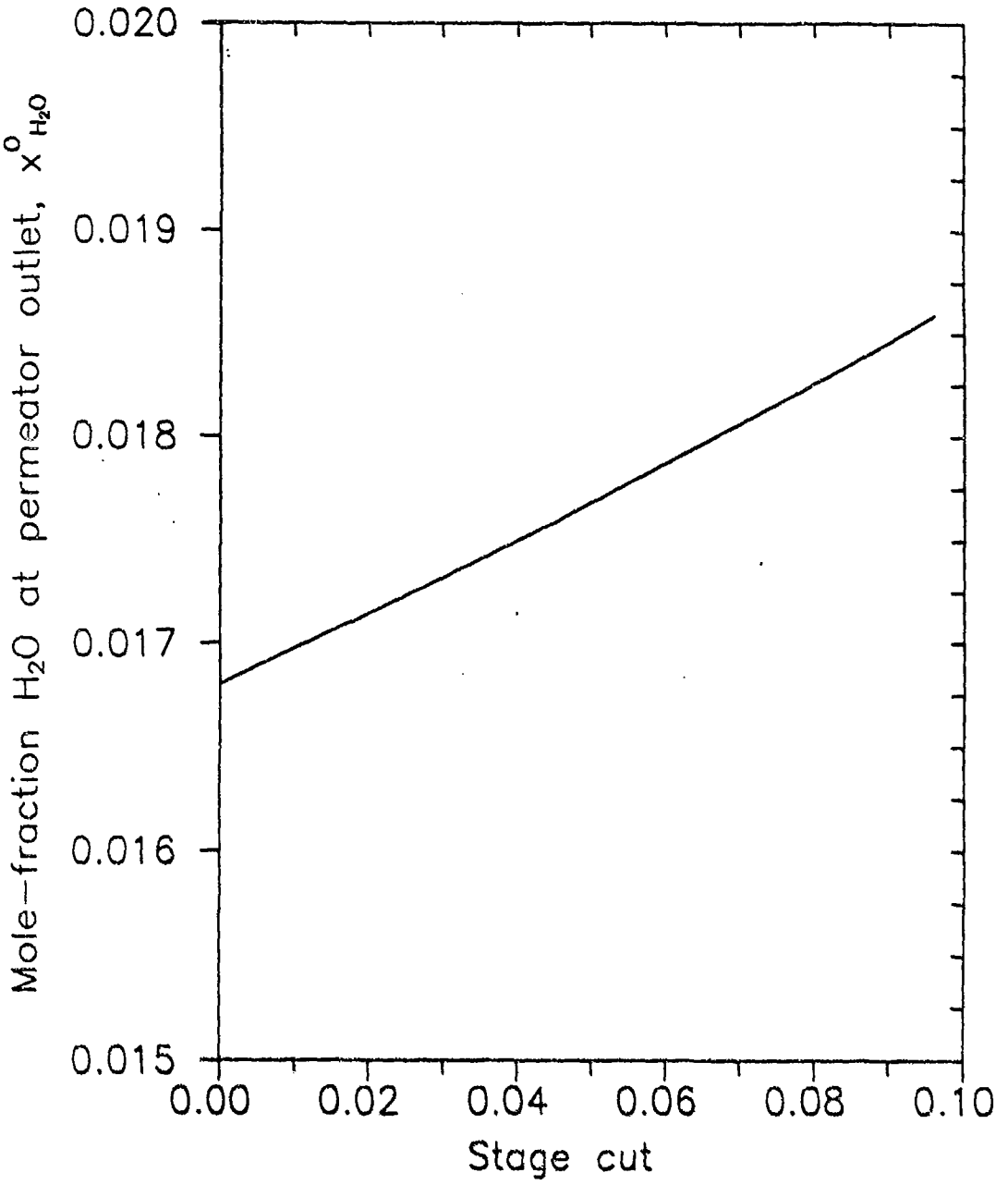

Figure 17: Water vapor concentration in exhaled air at permeator outlet as a function of stage cut. Membrane material - Acrylonitrile/butadiene copolymer.

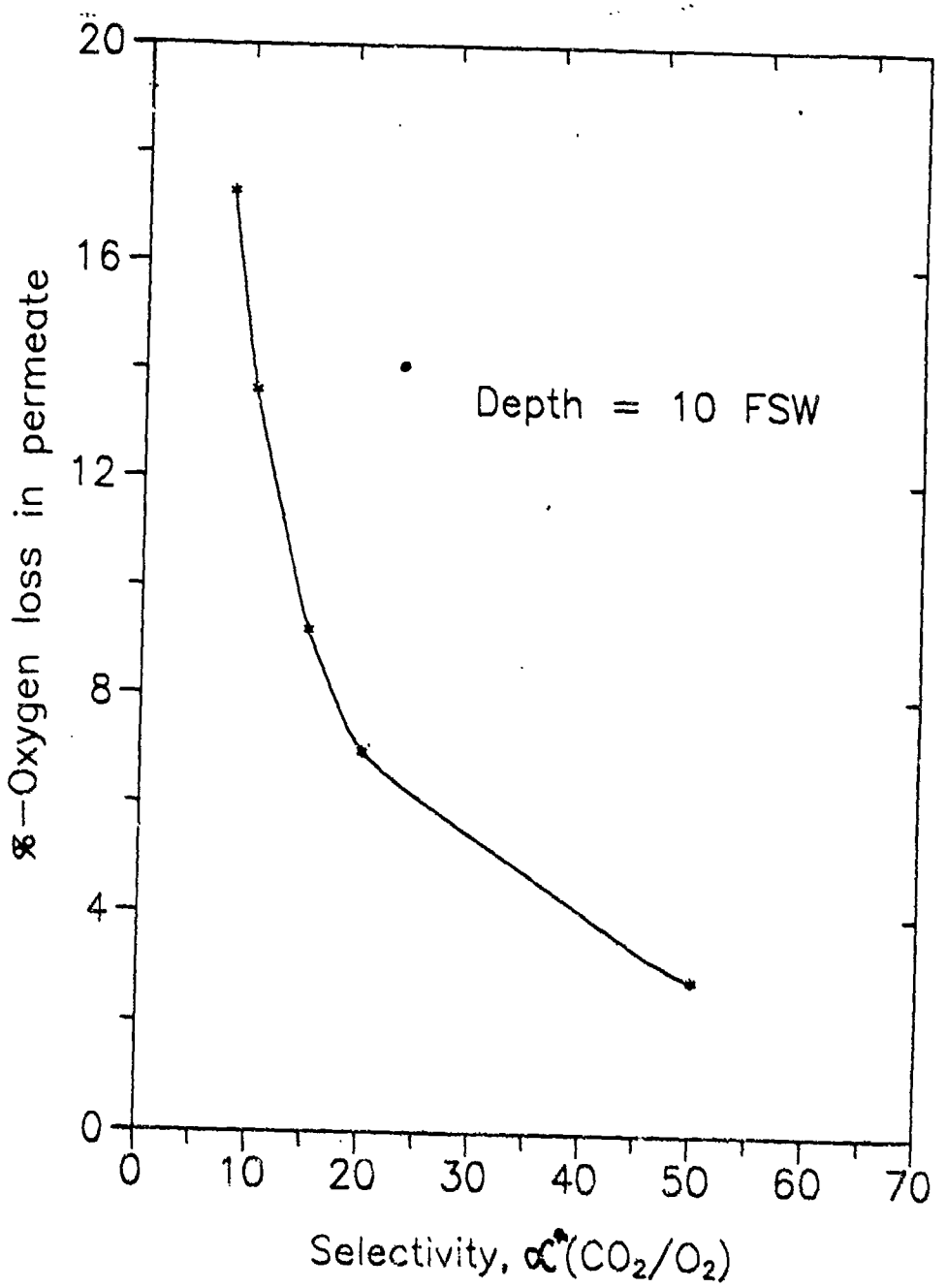

Figure 18: Effect of CO_2/O_2 selectivity of membrane on percent oxygen loss in permeate. The membrane permeability to CO_2 is assumed to be the same as that of ethyl cellulose: $P_{CO_2} = 113 \times 10^{-10} cm^3(STP) \cdot cm/(S \cdot cm^2 \cdot cmHg)$

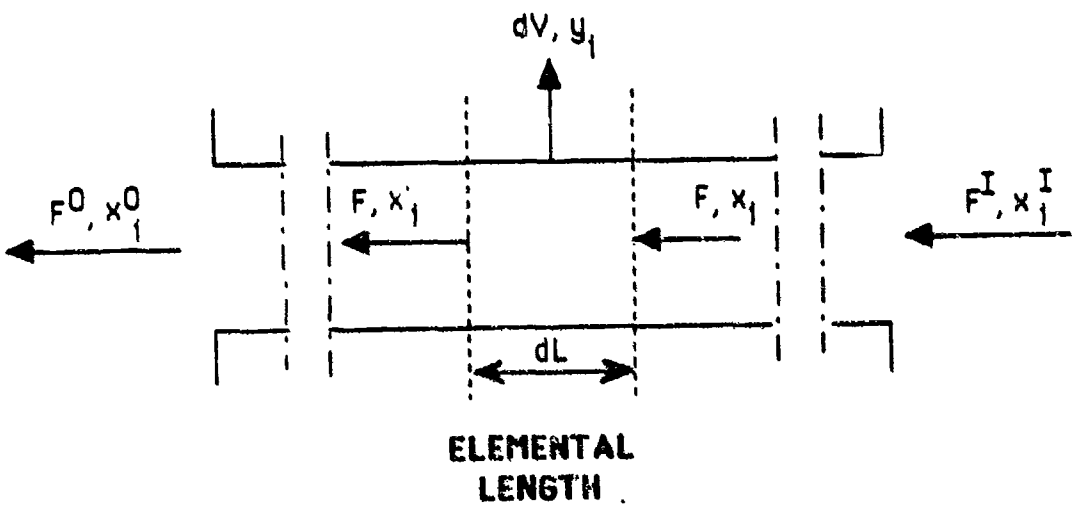

Figure 19: Enlarged section of a single hollow fiber showing the local variables.

APPENDIX I

TITLE: SIMULATION OF PERMEATOR MODULE OPERATING IN CROSS-FLOW MODE

Process simulations were performed using the "cross-flow" model, which was described earlier, cf. Figure 3. It was desired to calculate the membrane area required and the oxygen lost in the permeate when different amount of CO_2 are removed from exhaled air, which is then recycled to the breathing mixture. The membrane area required for the desired CO_2 separation then determines the size of the permeator module for CO_2 removal to be attached to the UBA.

The known and unknown quantities in this model are listed below.

Known quantities:

1. Feed flow rate,
2. Mole-fraction of each component in the feed (exhaled air),
3. Mole-fraction of CO_2 in the treated air stream at the permeator outlet, and
4. Permeability of membrane to each component of permeating gas mixture.

Unknown quantities:

1. Membrane area required for the desired removal of CO_2,
2. Pressure drop in hollow fibers, and
3. Oxygen lost in permeate to the sea water.

In order to calculate the unknown quantities listed above, it is necessary to formulate a system of relations comprising material balances and transport equations pertinent to cross-flow conditions in a permeator module.

Assuming a constant density for all gas streams, an overall mass balance over the permeator yields, cf. Figure 3:

$$F^I = F^0 + P^0 \qquad (I\text{-}1)$$

Similarly, a component mass balance yields:

$$F^I x_i^I = F^0 x_i^0 + V^0 y_i^0 \qquad \text{(I-2)}$$

where:

F^I = flow rate of exhaled air (the "feed") at permeator inlet,

F^0 = flow rate of treated air at the permeator outlet,

V^0 = net flow rate of permeate gas (the "permeate"),

x_i^I = mole fraction of component i in exhaled air at permeator inlet,

x_i^0 = mole fraction of component i in treated air at permeator outlet,

y_i^0 = mole fraction of component i in permeate.

At any point in the permeator, the net flow of gas through the wall of an element of length dL of a hollow fiber is given by the relation, cf. Figure 19:

$$dq_i = \pi d_o \, dL \, \left(\frac{D_i}{\delta}\right) \left(c^M_{F,i} - c^M_{P,i}\right) \qquad \text{(I-3)}$$

where:

dq_i = volume in cm^3(stp) of component i permeated per unit time,

$c^M_{F,i}$ = concentration of component i at any point in membrane at the membrane/feed interface,

$c^M_{P,i}$ = concentration of component i in membrane at the sea water/membrane interface,

d_o = outer wall diameter of the hollow fiber membrane effective dense skin thickness,

D_i = mean mutual diffusion coefficient of component i in polymer membrane (assumed constant),

dL = element of length of hollow fiber membrane.

The concentration of component i dissolved in the membrane at the feed/membrane interface is given by the expression:

$$c^M_{F,i} = S_i (p_h \cdot x_i) \qquad \text{(I-4)}$$

where:

S_i = solubility coefficient of component i in the membrane (assumed constant),

p_h = pressure of exhaled air on the feed side of the permeator module, i.e., inside the hollow fibers,

x_i = mole fraction of component i at any point in the feed (exhaled air),

$p_h \cdot x_i$ = partial pressure of component i at any point in the feed.

The concentration of component i dissolved in the membrane at the sea water/membrane interface is controlled by two factors:

a. The solubility of component i in sea water, and

b. The partition coefficient of component i between the membrane and sea water.

If $c^{SW}_{P,i}$ is the concentration of component i in sea water, it is possible to express $c^{SW}_{P,i}$ at the sea/atmosphere interface as a function of p_i, the partial pressure of component i in the atmosphere

$$c^{SW}_{P,i} = H_i \, p_i = H_i (p_{atm} \cdot y_{i,atm}) \qquad \text{(I-5)}$$

where:

p_{atm} = atmospheric pressure,

$y_{i,atm}$ = mole fraction of component i in ambient air,

H_i = solubility coefficient within the Henry's law limit.

Equation (I-5) describes the equilibrium between ambient air and sea water. In order to calculate the concentration of each species in the membrane at the sea water/membrane interface, it is necessary to consider the equilibrium of each component between the membrane and the sea water. This equilibrium can be expressed in terms of a partition coefficient of the component between the membrane and sea water. Thus, one can write,

$$c^{M}_{p,i} = K_i \cdot c^{SW}_{P,i} \quad , \qquad \text{(I-6)}$$

where:

K_i = partition coefficient of component i between sea water and membrane.

Substituting eqn. (I-5) into eqn. (I-6), one obtains,

$$c^{M}_{p,i} = K_i \cdot H_i (p_{atm} \cdot y_{i,atm}) \quad . \tag{I-7}$$

Also, substituting eqns. (I-5) and (I-6) into eqn. (I-3), we obtain:

$$dq_i = \pi d_o \, dL \, (\frac{D_i}{\delta}) \left[S_i p_h x_i - K_i H_i p_{atm} \cdot y_{i,atm} \right] . \tag{I-8}$$

The above equation can be rearranged to the form:

$$dq_i = (\pi d_o \, dL)(\frac{D_i S_i}{\delta}) \left[p_h x_i - \frac{K_i H_i}{S_i} p_{atm} \cdot y_{i,atm} \right] . \tag{I-9}$$

In eqn. (I-9), $d_o dL$ = dA = incremental area of membrane through which permeation occurs. Substituting the above relation in eqn. (I-9), one gets,

$$J_i = \frac{dq_i}{dA} = (\frac{P_i}{\delta}) \left[p_h x_i - \frac{K_i H_i}{S_i} p_{atm} \cdot y_{i,atm} \right] \tag{I-10a}$$

P_i = mean permeability coefficient of component i in the membrane = $D_i S_i$.

In eqn. (I-10a), the second term within the bracket represents the concentration of component i in the membrane "skin" in terms of pressure units. This can be rewritten in a more simple form by substituting:

$$K_i' = \frac{K_i H_i}{S_i} \quad . \tag{I-10b}$$

Substituting eqn. (I-10b) in eqn. (I-10a), one obtains,

$$J_i = \frac{dq_i}{dA} = (\frac{P_i}{\delta}) \left[p_h \cdot x_i - K_i' \, p_{atm} \cdot y_{i,atm} \right] \tag{I-10c}$$

where:

$p_h \cdot x_i$ = partial pressure of component i on the feed side.

The "stage cut" is the fraction of the feed permeating through th membrane and is defined by the relation:

$$\theta = V/F^{I} \quad , \tag{I-11}$$

where:

F^I = flow rate of feed at the inlet of permeator module

V = total permeated product at any distance L along the hollow fiber membranes from the inlet of the permeator module.

A mass balance over an increment of membrane area dA yields, cf. Figure 19:

$$-d(Fx_i) = J_i dA \qquad (I-12)$$

A summation for all i components in the feed yields, from eqn. (I-12),

$$-d(F\{x_1+x_2+...\}) = (J_1+J_2+....)dA, \qquad (I-13)$$

where x_1, x_2, x_3 .... are the mole-fractions of the i components at any distance L from the inlet of the permeator module, and J_1, J_2, J_3 ... are the fluxes of each of the i components at the same distance L from the inlet.

The sum of the mole fractions of all the components in the feed at any distance L from the inlet must always be equal to unity, i.e.,

$$x_1 + x_2 + ... = 1 \qquad (I-14)$$

Rewriting eqn. (I-13) we obtain:

$$-dF = \Sigma J_i dA \qquad (I-15)$$

Rewriting the term $d(Fx_i)$ in the form:

$$d(Fx_i) = x_i dF + F dx_i, \qquad (I-16)$$

and substituting eqn. (I-12) and (I-15) into eqn. (I-16), one further obtains

$$\frac{dx_i}{dA} = \frac{(-J_i + x_i \Sigma J_i)}{F} \qquad (I-17)$$

Equation (I-15) can be rearranged in the form:

$$dF/dA = \Sigma J_i \qquad (I-18)$$

Dividing eqn. (I-17) by eqn. (I-18):

$$\frac{dx_i}{dF} = \frac{(J_i - x_i \Sigma J_i)}{(F \Sigma J_i)} \qquad (I-19)$$

Dividing the denominator of eqn. (I-19) by F^I and substituting eqn. (I-11), one obtains the relation:

$$\frac{dx_i}{d\theta} = \frac{-(J_i - x_i \Sigma J_i)}{(1-\theta)\Sigma J_i} , \qquad \text{(I-20)}$$

and from eqn. (I-14), one obtains

$$\frac{dA}{d\theta} = \frac{F^I}{\Sigma J_i} . \qquad \text{(I-21)}$$

Equations (I-19) and (I-20) are the two differential equations which must be solved simultaneously to obtain the membrane area and the concentrations of each component in the treated air at the outlet of the membrane permeator module. The boundary conditions are as follows:

The following conditions prevail at the inlet of the permeator module: V = 0 and the "stage cut" θ = zero, cf. eqn. (I-11). The membrane area is also zero at the inlet of the module, and the concentration of each component is equal to that in the feed (exhaled air), thus:

$$\theta = 0,$$

$$A = 0, \text{ and}$$

$$x_i = x_i^F$$

Equations (I-20) and (I-21) were solved using a 3rd order Runge-Kutta algorithm and the boundary conditions described above.

The other important design consideration is the pressure drop across the hollow fibers in the permeator. The pressure drop was calculated by means of the Hagen-Poiseuille equation (12). For the present calculations it was assumed that the flow rate of the feed was constant at all points from the inlet to the outlet of the permeator, and equal to that at the inlet of the permeator. However, in the actual case, the feed flow rate decreases along the permeator as permeation occurs. This implies that the pressure drop will

be lower than that calculated using this simplified equation. The temperature of sea water was assumed to be 25°C.

According to the Hagen-Poiseuille equation:

$$\Delta p_S = 32\ \mu L \frac{v}{d_i^2}\ , \qquad \text{(I-22)}$$

where

Δp_S = pressure drop in hollow fibers,

v = average velocity of feed in hollow fibers,

μ = viscosity of feed at sea water temperature,

L = length of hollow fibers,

d_i = internal diameter of hollow fibers.

The average velocity of the feed can be calculated as follows

$$v = \text{flow rate/cross-sectional area} = \frac{F^I 4}{(\pi d_i^2 N)}\ . \qquad \text{(I-23)}$$

The membrane area requirement is fixed by the desired separation:

$$\text{Membrane area required} = A_m = \Pi d_o L N\ . \qquad \text{(I-24)}$$

Rearranging eqn. (I-23), one obtains

$$N = \frac{A_m}{\pi d_o L}\ . \qquad \text{(I-25)}$$

Substituting eqns. (I-23) and (I-25) into eqn. (I-22), one obtains

$$\Delta p_S = \frac{128\ \mu L^2 D_o F^I}{D_i^4 \cdot A_m}\ (\text{dynes/cm}^2)\ . \qquad \text{(I-26)}$$

The pressure drop units can be converted to cms. of water by multiplying by 0.00102289. The viscosity of the feed was estimated to be 1.75×10^{-4} poise.

APPENDIX II

From "Synthetic Membranes", M. B. Chenoweth, Ed., MMI Press Symposium Series, Vol. 5, Harwood Academic Publishers, New York, 1986, pp. 1-37

New Developments in Membrane Processes for Gas Separations

S. ALEXANDER STERN

Development of Chemical Engineering and Materials Science Syracuse University, Syracuse, NY 13210

Membrane separation is now a well-established technology, particularly because of the variety of applications of reverse osmosis and membrane ultrafiltration. Some of these applications are on a substantial scale, such as in the desalination of brackish and sea water. Membrane separation has become economically competitive in these areas because of the development of high-flux asymmetric membranes and the ability to fabricate such membranes in the form of hollow fibers. In recent years, further progress in membrane science has resulted in the successful application of membrane technology to the separation of gases of industrial interest. A number of large-scale membrane plants for the separation of hydrogen from various industrial gas streams and for the recovery of carbon dioxide in extended oil recovery are presently in operation. These membrane processes are competitive with conventional gas separation techniques. The separation of several other important gases by selective membrane permeation, such as of oxygen from air, is being studied in many laboratories. It is anticipated that, in a not too distant future, competitive membrane processes will become available also for the separation of liquid mixtures, such as azeotropes and mixtures of organic compounds. The discussion will outline the engineering and economic factors affecting the development of membrane processes for the separation of both gases and liquids, and will summarize the state-of-the-art in these areas.

I. INTRODUCTION

The development of membrane processes for the separation of gas mixtures has made remarkable progress during the last two decades. The basic concept underlying this technology, namely, the selective permeation of gases through nonporous polymer membranes, appears to have first been proposed by Graham (1) as early as 1866. A full century later, in the early 1960's, membrane processes for gas separations were still being studied largely on a laboratory scale.

Today, over 100 membrane separation plants are in operation in the United States as well as in Europe and in Japan. Most of these plants are for the separation of H_2 from various industrial gas streams, such as in NH_3 and CH_3OH synthesis, in petroleum refining, and in petrochemical

operations. However, a number of membrane plants separate CO_2 in enhanced oil recovery (EOR), from natural gas, and from landfill gas, while a few plants separate air to produce 96% N_2 for the "inerting" (blanketing) of fuel tanks. The largest membrane separation plant, which was designed to separate CO_2 from mixtures with hydrocarbons in OER, has been reported to process 50×10^6 cu. ft. ($1.4 \times 10^6 m^3$) of feed gas/day (2). Many other membrane processes for the separation of gas mixtures are being studied at present both on a laboratory and pilot-plant scale, as can be seen from Table I. It has been estimated that the total available market for membrane separation processes could reach $500 million between now and 1990.

The great interest in membrane separation technology is due mainly to the fact that it is potentially energy-efficient. In addition, the required process equipment is simple, compact, and relatively easy to operate and control. Moreover, this equipment is modular and can be easily scaled up or operated by reduced capacity if necessary. Membrane separation became economically competitive in 1961, when Loeb and Sourirajan (3) developed their high-flux, asymmetric membranes of cellulose acetate for water desalination by reverse osmosis. Asymmetric membranes can now be made from many types of polymers, and are being employed for the separation of gases both in sheet form and in the form of composite hollow fibers. However, the greatest impetus to the development of membrane separation technology was given by the energy crisis of 1973, which occured just at the time when this technology had reached a significant degree of maturity.

The objective of the present paper is to summarize some of the charac-

TABLE I

Membrane processes for the separation of gas mixtures

H_2 from ammonia synthesis purge gas
H_2 from methanol synthesis purge gas
H_2 from hydrodesulfurizer purge gas
H_2 from hydrogenator purge gas
H_2 from petrochemical synthesis gas
O_2 and N_2 from air
CO_2 separation in enhanced oil recovery
CH_4 from biomass, landfill, coal mine, and oil field gases
CH_4 from low BTU (CO_2- and N_2-rich) natural gas
He recovery from natural gas
CO_2 and H_2S scrubbing of acid gases
Dehydration of natural gas and of industrial gases
Separation of Kr and Xe from nuclear reactor atmospheres

teristics of membrane processes for the separation of gas mixtures, and to highlight new and promising developments in this field.

II. MECHANISM OF GAS PERMEATION

It is generally accepted that gases permeate through nonporous polymer membranes by a "solution-diffusion" mechanism (4–8). This mechanism can be described with reference to Figure 1, which shows a cross-section through a planar membrane. Application of gas pressure at one interface of such a membrane results in the following sequence of events: (1) solution (absorption) of the gas into the membrane at that interface, (2) molecular diffusion of the gas in and through the membrane, and (3) release of the gas from solution (desorption) at the opposite interface. The term *permeation* is accordingly used to describe the overall mass transport ~~of transport~~ of "penetrant" gas across the membrane, whereas the term *diffusion* refers only to the movement of gas molecules inside the polymer matrix.

In most cases of interest in membrane separations, molecular diffusion is the slowest and, hence the rate-determining step in the permeation process. By contrast, the absorption and desorption steps are so fast that solution equilibrium is usually established at the membrane interfaces. Diffusion of a gas in and through a polymer membrane can usually be described by Fick's two laws. By solving Fick's laws for the desired physical conditions, i.e., for the appropriate initial and boundary conditions, it is possible to formulate the rate of diffusion J as well as the penetrant concentration profile within the membrane. J is also the rate of gas permeation through the membrane since, as mentioned above, diffusion is rate controlling. Crank (8) and Jost (9) have described various methods of solving Fick's equations for different membrane geometries and boundary conditions, for constant and variable diffusion coefficients, and for both transient and steady-state transport.

From a practical viewpoint, it is of interest to determine the rate of gas permeation under *steady-state* conditions, J_s, as well as the dependence of this rate on pressure and temperature. Steady-state is achieved if, at a given temperature, the constant pressures p_h and p_ℓ ($<p_h$) are maintained at the two membrane interfaces, respectively. For example, the following expression can be derived from Fick's first law for the steady-state rate of gas permeation through a planar, isotropic, and homogeneous membrane of thickness δ (4, 5):

$$J_s = \bar{P}(p_h - p_\ell)/\delta, \qquad (1)$$

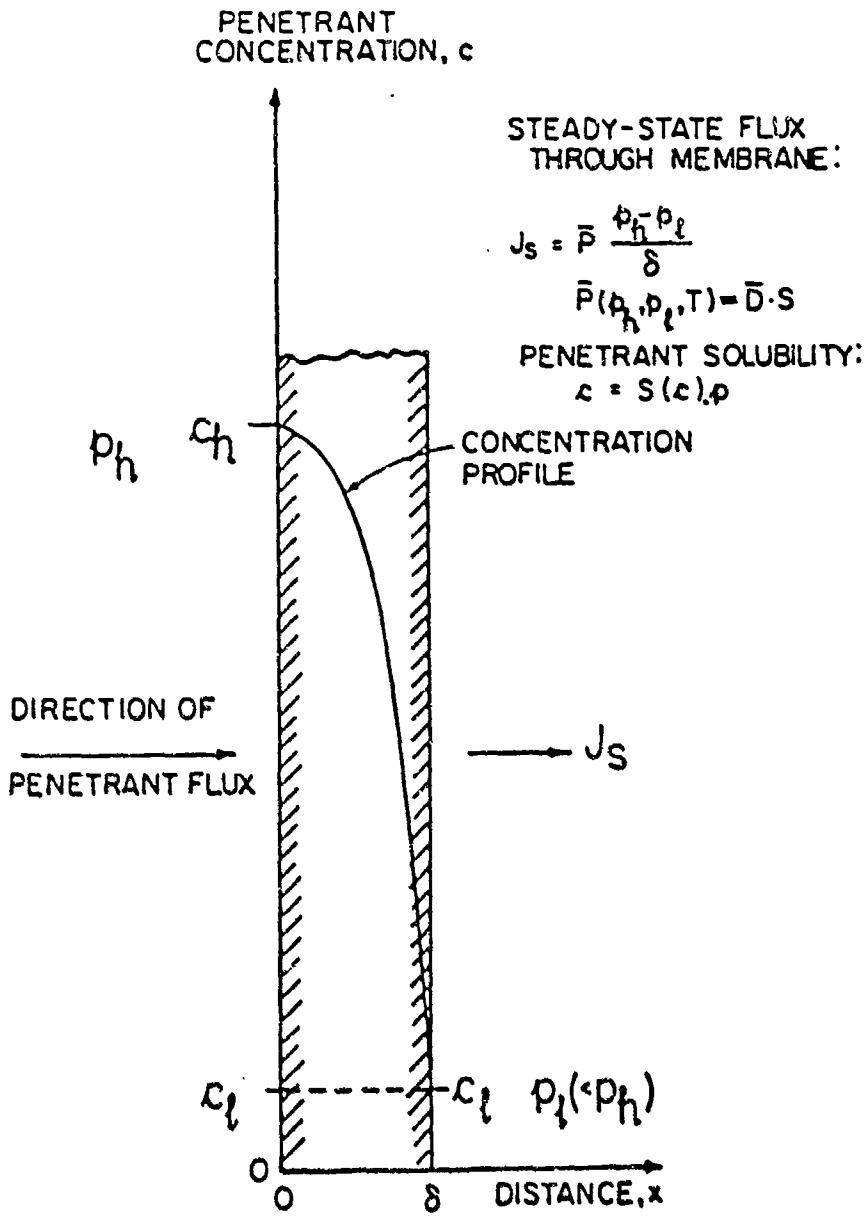

FIGURE 1 "Solution-diffusion" mechanism of gas permation. Cross-section of a non-porous polymer membrane.

where $\bar{P}$ is a mass-transfer coefficient known as the mean "permeability coefficient" or the "permeability"; eqn. (1) refers to a specified temperature and unit area of membrane.

It can be further shown that when $p_h \gg p_\ell$, as is the case in membrane separation processes, the permeability coefficient $\bar{P}$ is a product of a mean diffusion coefficient $\bar{D}$ and a solubility coefficient S_h:

$$\bar{P} = \bar{D} \cdot S_h, \tag{2}$$

where

$$\bar{D} = \frac{\int_{c_\ell}^{c_h} D(c)dc}{(c_h - c_\ell)},$$

$$S_h = c_h/p_h, \tag{4}$$

and where c_h and c_ℓ are the equilibrium concentrations of penetrant dissolved at the two membrane interfaces when the penetrant pressures at these interfaces are p_h and p_ℓ, respectively; and $D(c)$ is the mutual diffusion coefficient for the penetrant/membrane system. In the most general case, $\bar{P}$ depends on the nature of the penetrant and the polymer membrane, on both p_h and p_ℓ, and on the temperature.

Similarly, it can be shown that the steady-state rate of gas permeation through a tubular membrane, such as a capillary or hollow fiber, is given by the relation:

$$J_s = \bar{P}\frac{2\pi L(p_h - p_\ell)}{\ln(R_0/R_\ell)}, \tag{5}$$

where R_0 and R_ℓ are the effective outer and inner radii of the tube, and L is the length of the tube.

The rate of permeation of a component of a gas mixture is also given by eqns. (1) or (5), but the permeability coefficient $\bar{P}$ may then be a function of composition as well, where p_h and p_ℓ are then the *partial* pressures of that component of the two membrane interfaces.

The *selectivity* of a nonporous membrane toward two different components A and B of a permeating gas mixture is usually expressed in terms of an ideal separation factor, α^*, which is defined by the relation(s):

$$\alpha^*(A/B) = \bar{P}^A/\bar{P}^B \tag{6}$$

If the membrane exhibits a higher selectivity for component A than for B (i.e. at equal partial pressures, A permeates faster through the membrane than B) then $\alpha^*(A/B) > 1$, whereas the opposite is true if $\alpha^*(A/B) < 1$. No separation can occur, of course, when $\alpha^*(A/B) = 1$. The ideal separation factor is, therefore, a separation index similar to the relative volatility used in distillation.

III. PRINCIPLES OF MEMBRANE PROCESS DESIGN

A. General Considerations

Gas mixtures are separated by selective permeation through a polymer membrane in devices known as "permeators". The permeator is the basic membrane separation unit, or stage, and consists essentially of a high-pressure vessel containing a large area of membrane. The vessel is provided with an inlet for the gas mixture to be separated (the "feed") and outlets for two or more product streams. Additionally, the permeator is provided with the necessary piping and valving, and with instrumentation for the control and measurement of flow rates, pressures, and temperature. The compositions of the feed and product streams are also monitored.

The operation of a conventional permeator is illustrated in Figure 2, where the permeator is represented conceptually as a "black box" separated into two compartments by a planar membrane. The feed stream flows through one of the compartments at some suitable pressure p_h, which is usually maintained constant. The opposite compartment is maintained at some lower constant pressure, p_ℓ. A fraction of the feed, known as the "stage cut", is allowed to permeate through the membrane into the low-pressure compartment. The feed stream is thereby separated into two product streams: (a) a permeated (low-pressure) stream enriched in the faster permeating components of the feed, and (b) an unpermeated (high-pressure) stream depleted in these components. The magnitude of the stage cut will depend on the feed flow rate, the membrane area, and the pressure ratio $r = p_h/p_\ell$.

It should be noted that the membrane need not be planar, or in sheet form, as is shown in Figure 2, but can also be, and most often is in the form of a bundle of hollow fibers or capillaries. A diagram of a hollow fiber permeator is shown in Figure 3, where the high- and low-pressure streams are represented as flowing countercurrently to one another. It is seen that a hollow fiber permeator greatly resembles a tubular heat exchanger.

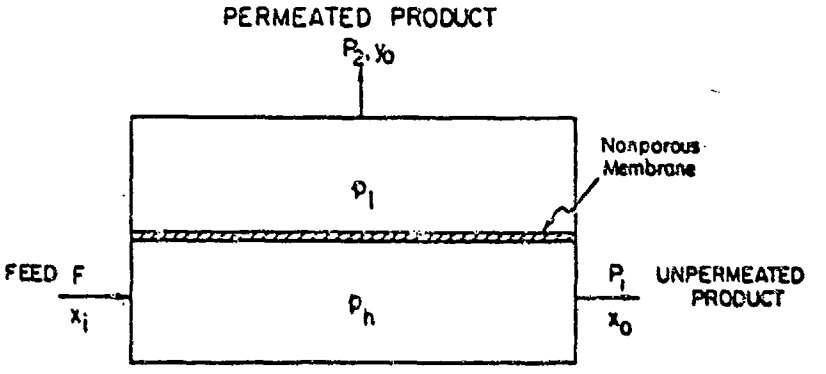

FACTORS AFFECTING PRODUCT COMPOSITIONS AND MEMBRANE AREA

1) Feed Composition
2) Nature of Membrane
3) Temperature
4) Pressures p_h and p_l ($< p_h$)
5) Stage Cut θ ($= P_2/F$)
6) Flow Patterns on High- and Low-Pressure Sides of Membrane

FIGURE 2 Diagram of permeator (single permeation stage).

Given the composition of the feed stream, the process designer must select a membrane with a suitable gas selectivity and permeability. He may be guided in this task by the criteria discussed in a following section. The process designer then wishes to determine the compositions of the product streams and the membrane area requirement for various operating conditions. The extent of separation achievable in a permeator (i.e. in a single permeating stage), and hence the compositions of the product streams, will depend on the following factors (5, 10–12), cf. Figure 2:

Feed composition
Nature of the membrane
Pressures p_h and p_l

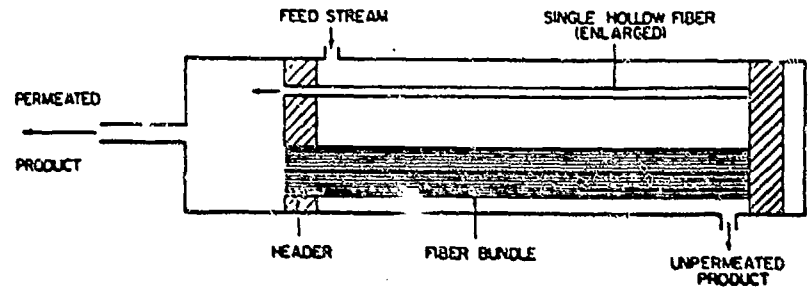

FIGURE 3 Hollow-fiber permeator.

Temperature
Stage cut
Flow patterns of the high- and low-pressure streams in the permeator.

The flow rates of the product streams are determined by the feed flow rate, and by the selected stage cut and pressure ratio $r(=p_h/p_l)$. The membrane area also depends on the above factors as well as on the feed flow rate.

The first four factors listed above are expressed by the permeability coefficient $\bar{P}$, whose numerical value must be determined experimentally for the desired conditions or predicted, if possible from suitable correlations. The effects of the last two factors are discussed below.

B. Effect of Stage Cut

Consider the membrane separation of a binary gas mixture of components A and B, where A is assumed to be the more rapidly permeating component. The effect of the stage cut θ on the composition of the permeated product stream (the "permeate") is illustrated in Figure 4 for a hypothetical separation process. The stage cut θ is the fraction of the feed permeating through the membrane; thus, if F, P_1, and P_2 are the total flow rates of the feed, unpermeated, and permeated streams, respectively, then $\theta = P_2/F$.

It is seen from Figure 4 that, for specified values of $\alpha'[=\bar{P}(A)/\bar{P}(B)]$ and of $r(=p_h/p_l)$, the highest concentration of component A in the permeate is obtained in the limit $\theta \to 0$, i.e. when an infinitesimal fraction of the feed permeates through the membrane. As θ is increased, the concentration of A in the permeate decreases. When $\theta = 1$, the other

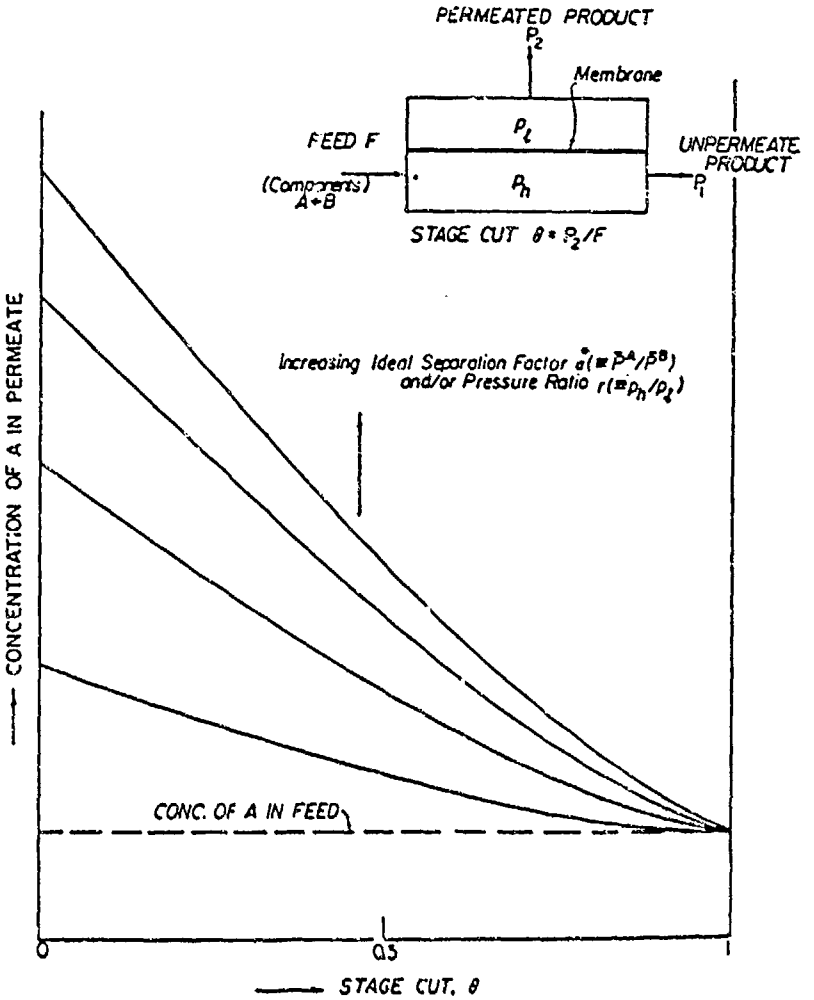

FIGURE 4 Effect of "stage cut" on permeate composition. More permeable component: A($P^A > P^B$).

limit, no separation is obtained because *all* the feed is forced through the membrane ($P_2 = F$).

The process designer is thus faced with an optimization problem. In order to increase the concentration of component A in the permeate (at a given α^* and r) he must decrease θ, thereby decreasing also the permeate flow rate, and vice versa. At a given θ, the concentration of A in the permeate can be increased by increasing α^* or r, or both these para-

meters. The value of α^* depends on the chemical composition and morphology of the membrane. The possibility of increasing α^* for a given pair of penetrant gases depends, therefore, on the ability of polymer chemists to synthesize more highly gas-selective membranes. The value of the pressure ratio r is usually limited by economic considerations.

C. Effect of Flow Pattern

The extent of separation achievable in a single permeator and the required membrane area depend also on the flow patterns of permeated and unpermeated gas streams, relative to one another, in the permeator (5, 10–12). Four such patterns, for "perfect mixing", cross flow, concurrent flow, and countercurrent flow, are illustrated diagrammatically in Figure 5.

In the "perfect mixing" case it is assumed that the unpermeated high-pressure) gas stream in the permeator is mixed so rapidly that its com-

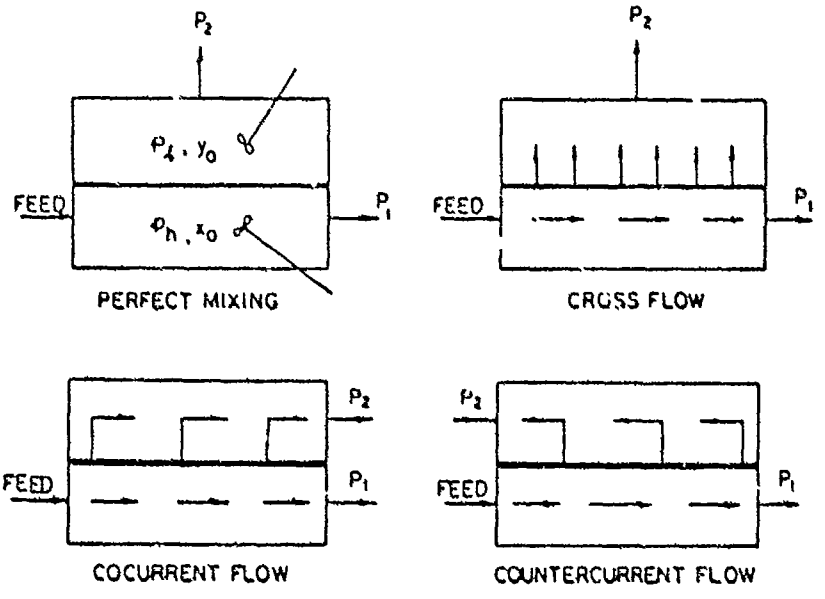

FIGURE 5 Flow patterns in single permeation stage. P_1 = Unpermeated Product; P_2 = Permeated Product.

position at *all points* in the permeator is the same as that at the permeator outlet. The same assumption is made for the permeated (low-pressure) stream. A step-wise change in the feed composition occurs here at the permeator inlet, as is the case in the ideal continuous stirred tank reactor (CSTR). The other flow patterns illustrated in Figure 5 are self-explanatory. In these cases, the composition of both the permeated and unpermeated streams vary continuously from the inlet to the outlet of the permeator, both streams becoming depleted in the more rapidly permeating component(s).

The effect of the flow pattern in a permeator on the separation of a hypothetical mixture of components A and B is shown as a function of stage cut in Figure 6. The plot is for given values of α^* and of the pressure r, and A is again assumed to be the more rapidly permeating component. As is indicated in Figure 6, countercurrent flow is the most efficient flow pattern at any given stage cut $0 < \theta < 1$, in that it yields the highest concentration of A in the permeate. It can also be shown that countercurrent flow requires the smallest membrane area. By contrast, "perfect mixing" is the least efficient flow pattern in these respects. Other flow patterns yield intermediate results.

The difference in the effects of the above flow patterns on the extent of separation and membrane area requirements is more pronounced the larger the values of α^* and r. However, all flow patterns yield the same results in the stage-cut limits $\theta \to 0$ and $\theta \to 1$.

The factors affecting the separation of gas mixtures by selective permeation are now well understood. The performance of permeators can be predicted with confidence for any desired operating conditions from suitable mathematical models (5, 10, 13–24), if the pertinent permeability coefficients are known.

IV. NEW CONCEPTS IN MEMBRANE PROCESS DESIGN

A. Motivation

At the present time, the number of membrane processes for gas separations which are economically viable is very limited because of the lack of membranes with a sufficiently high selectivity and permeability toward a spectrum of different gases. This situation is not surprising since most available membranes of commercial origin were developed for purposes other than for gas separation, e.g. for packaging. Considerable work aimed at the synthesis of more highly gas-selective membranes for a variety of separation processes is currently in progress in many labor-

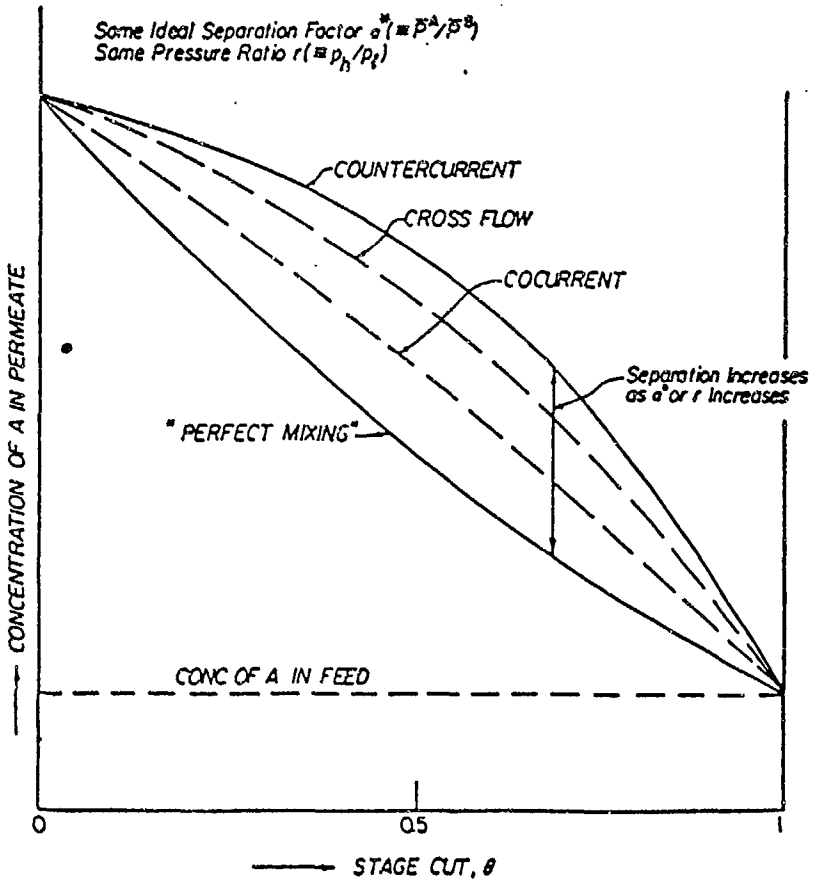

FIGURE 6 Effect of "stage cut" on permeate composition for different flow patterns. More permeable component: $A(\bar{P}^A > \bar{P}^B)$.

atories. However, the extent of separation that can be achieved in a membrane process can also be considerably enhanced in some cases by several process design techniques, using already available membranes.

A well-established technique of increasing the extent of separation in a membrane process is to connect two or more permeators *in series* to form a countercurrent cascade, cf. Figure 7. The permeated stream from each permeator is recompressed and used as feed for the succeeding permeator,

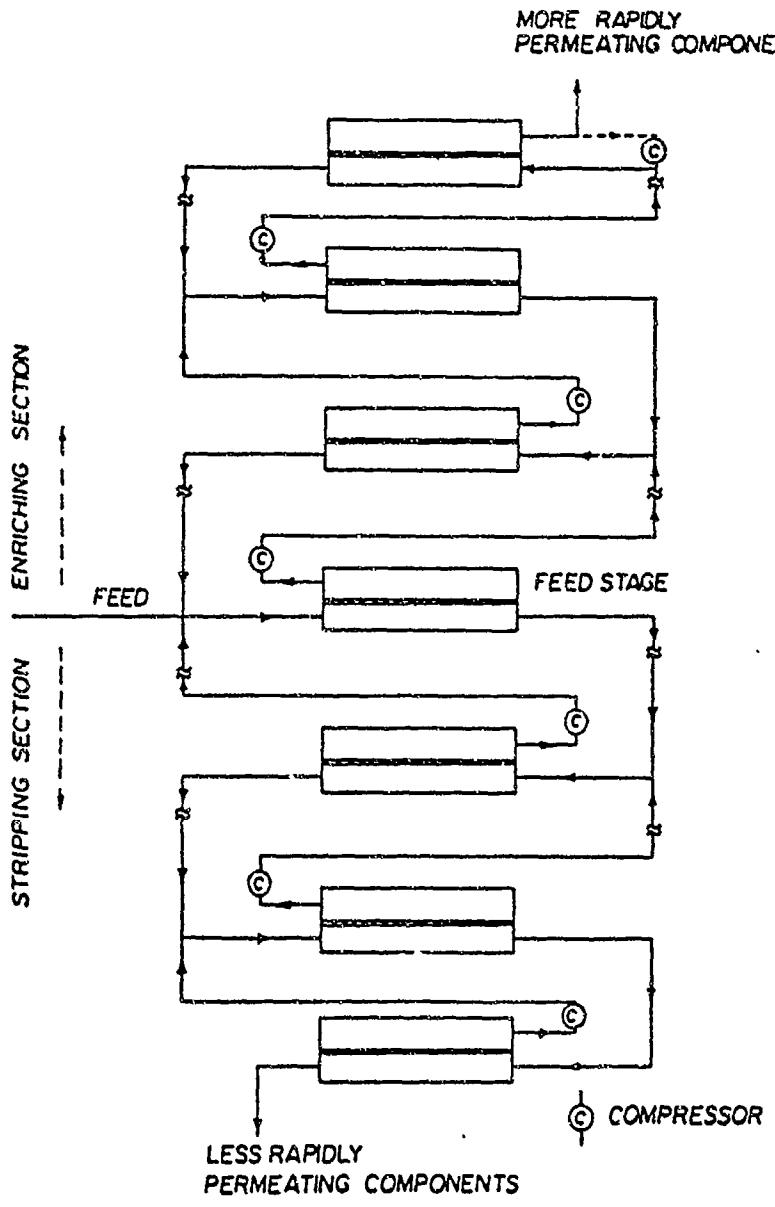

FIGURE 7 Countercurrent permeation cascade.

while the unpermeated stream is returned and mixed with the feed to the preceding permeator. Large cascades using porous barriers as separation elements are presently used in several countries for the separation of uranium isotopes by gaseous diffusion. The principles of cascade design, as applied to the separation of gas mixtures with nonporous polymer membranes, have been discussed by a number of investigators (5, 25).

Economic evaluations show that, with few exceptions, permeation cascades are not competitive with conventional separation techniques even if only two permeators in series are required. Of course, a number of permeators can always be connected *in parallel* in order to increase product output. Two relatively new concepts in membrane process design, which are discussed below, may prove to be more economical than the staging of permeators in cascades. These concepts involve (1) the use of various product recycling techniques, and (2) the use of two (or more) different types of membrane in a permeator, each type being selective to a different component of a feed mixture (26). A special recycle permeator known as the "continuous membrane column" deserves special consideration. The use of a "purge" or "sweep" gas on the permeate side of a permeator is also discussed.

B. Recycle Permeators

A potentially efficient method of enhancing the extent of separation is to recycle a fraction R of the permeated product stream into the feed stream as shown in Figure 8. The effect of product recycling is illustrated qualitatively in Figure 9 for a hypothetical binary mixture and membrane. The figure shows the concentration of the more rapidly permeating component of the mixture, A, in the permeate as a function of the *overall* stage cut $\theta = (1 - R)P_2/F$ and for various values of R. For $R = 0$, i.e., for the case where the permeator is operated without recycle, one obtains the usual permeation behavior described earlier: the maximum concentration of A is obtained when $\theta \rightarrow 0$, while no separation is achieved when $\theta \rightarrow 1$. For a given flow pattern (e.g., countercurrent), the concentration of A will increase with increasing ideal separation factor α^*. When part of the permeated products is recycled to the feed ($0 < R < 1$), the concentration of A in the plots of Figure 9 is seen to increase with increasing R above the values obtainable without product recycle ($R = 0$) for the same α^* and r. For large recycle fractions, R, the plot of concentration of component A in the permeated product tends to develop a sharp maximum as R is increased.

The effectiveness of recycling is illustrated quantitatively in Figure 10

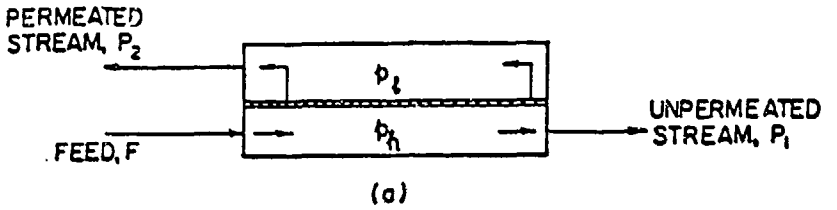

(a)

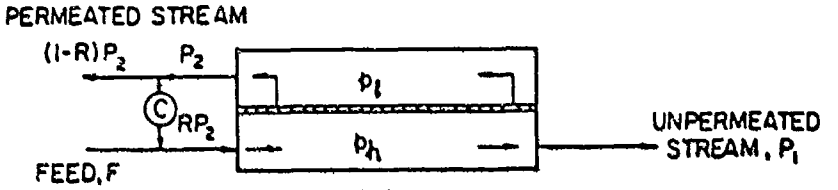

(b)

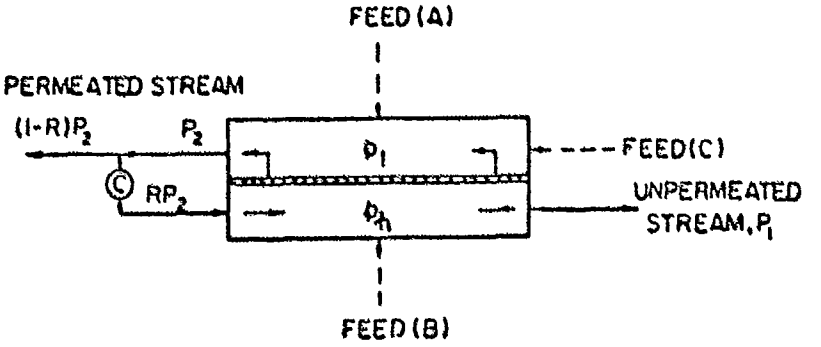

(c)

FIGURE 8 Recycle permeators (a) Permeator without permeate recycling; (b) Recycle permeator; (c) Feed inlet points in recycle permeator.

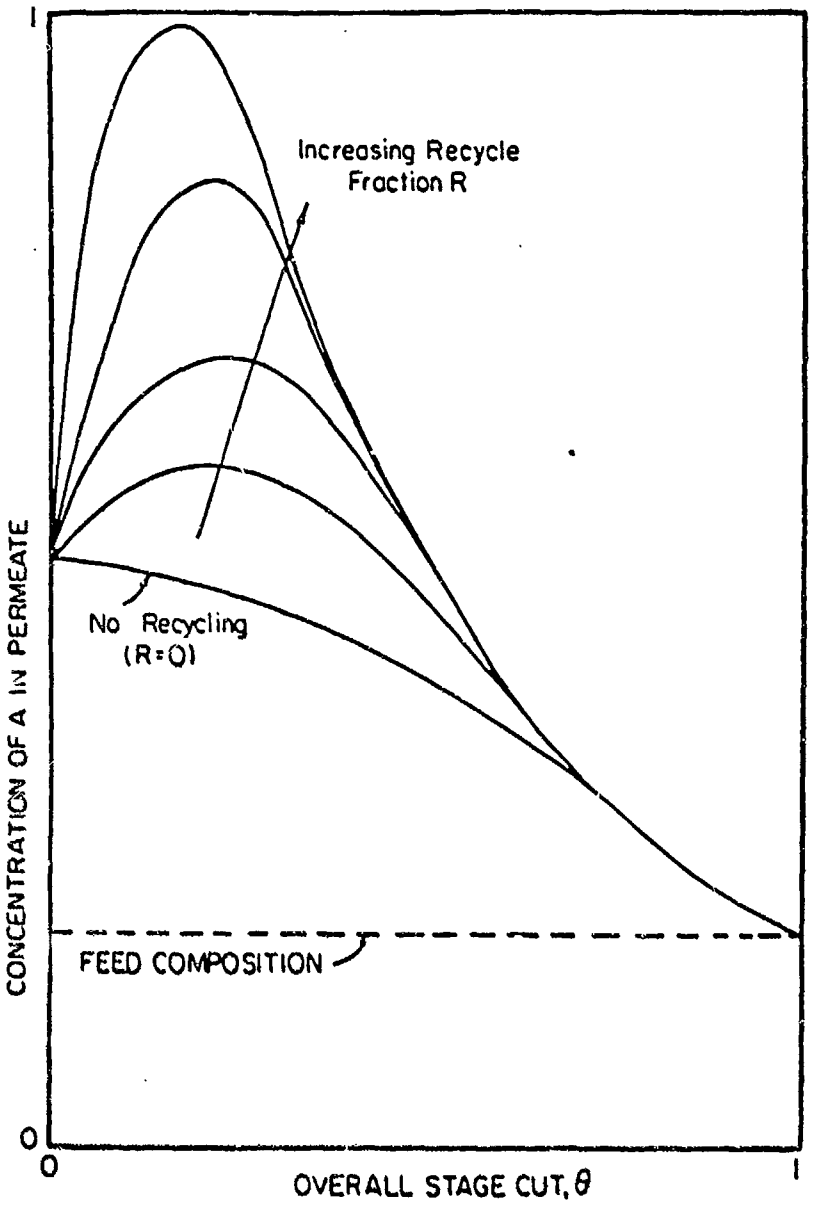

FIGURE 9 Effect of "stage cut" and permeate recycle fraction on permeate composition. More permeable component: $A(P^A > P^B)$.

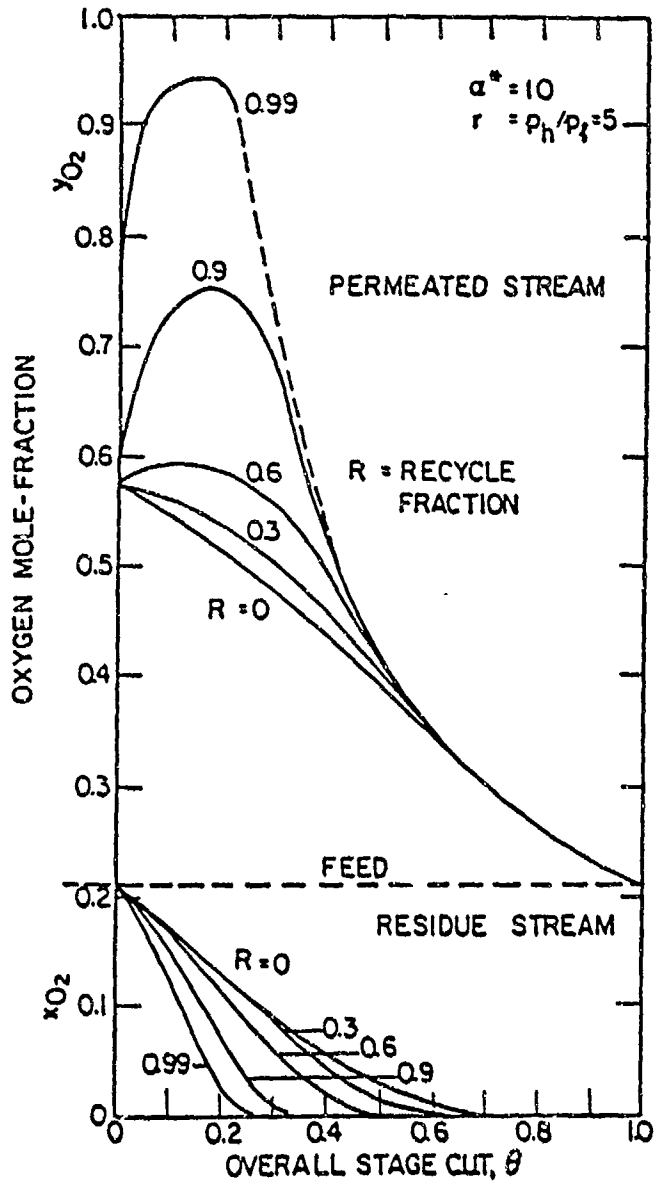

FIGURE 10 Air separation in a recycle permeator. Effect of overall "stage cut" on permeate composition. Countercurrent Flow.

for the case of air separation. In this example, air is taken to be a binary mixture of 20.9 mol % O_2 and 79.1 mol % N_2. It is also assumed that a membrane with an ideal separation factor, $\alpha^*(O_2/N_2)$, of 10 is used and that the pressure ratio r is 5; the assumed value of α^* cannot be obtained with any of the solid polymer membranes available at present, but should be achievable with some "facilitated transport" membrane. Figure 10 shows that the O_2 concentration in the permeated product stream passes through a maximum at a stage cut $\theta = 0.1-0.3$ when $R \gtrsim 0.6$, and that this maximum increases very rapidly with increasing R values. However, the power and capital investment costs of the permeation process also increase very rapidly with increasing R, because of the increase in the volume of gas recycled and in membrane area requirements (see Figure 11).

C. The Continuous Membrane Column

An examination of Fig. 8 suggests that the feed stream need not be introduced into the permeator at the recycle end of the stage, as is shown in that figure. The feed can be inserted anywhere between the two ends of the permeator, either in the high-pressure or low-pressure compartment, as illustrated in Figure 8 (feed locations A or B). In such cases, the permeator is transformed into a membrane separation device sometimes called a "continuous membrane column" (CMC), which is shown in more detail in Figure 12a. This device was apparently first described by Pfefferle (27), and has been studied in recent years by Hwang and coworkers (e.g., (28)).

Referring to Figure 12a, the CMC is seen to consist of an enriching section and a stripping section, not necessarily of the same length. The product streams can be recycled both at the top and the bottom of the CMC. The roles of the enriching and stripping sections are the same as those in distillation columns, namely, to obtain the maximum separation as well as recovery of a desired component from the feed mixture.

The principle of operation of the CMC is somewhat similar to that of a thermal diffusion column: the local separation of a gas mixture due to permeation (or thermal diffusion) at any point in the column may be small, but this elementary separation is multiplied many times as the gas mixture flows axially toward the ends of the column. The more rapidly permeating component is concentrated on the low-pressure side of the CMC in the low-pressure gas stream.

The extent to which a gas mixture can be separated in a CMC will depend on the recycle fraction R for a given membrane (i.e. for a given

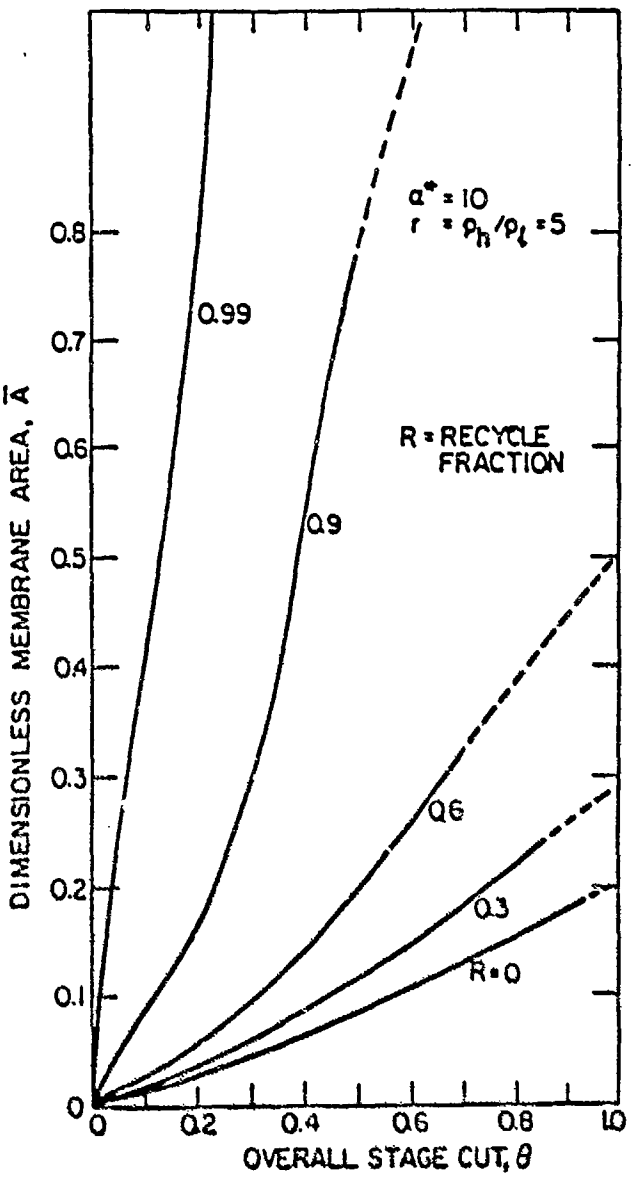

FIGURE 11 Air separation in a recycle permeator. Effect of overall "stage cut" on membrane area requirements. Countercurrent Flow.

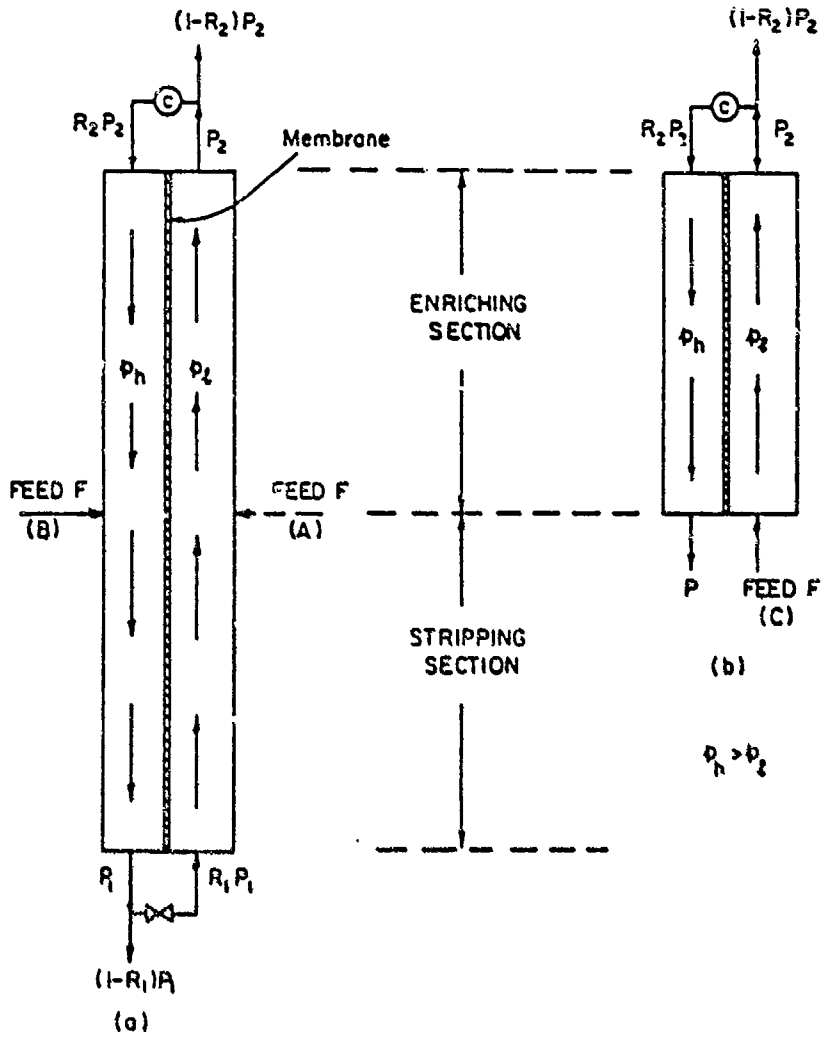

FIGURE 12 The continuous membrane column.

α^*), on the pressure ratio r, and on the stage cut θ. Typical results are shown in Figure 13 for the separation of air, assuming that α^* $(O_2/N_2) = 10$ and $r = 5$. The feed (air) is inserted on the high-pressure side of the CMC and at column pressure, at a point where the gas in the CMC has the same composition as the feed.

It is seen from Figure 13 that the concentration of O_2 in the permeated product stream does not exhibit a maximum as was the case in the recycle

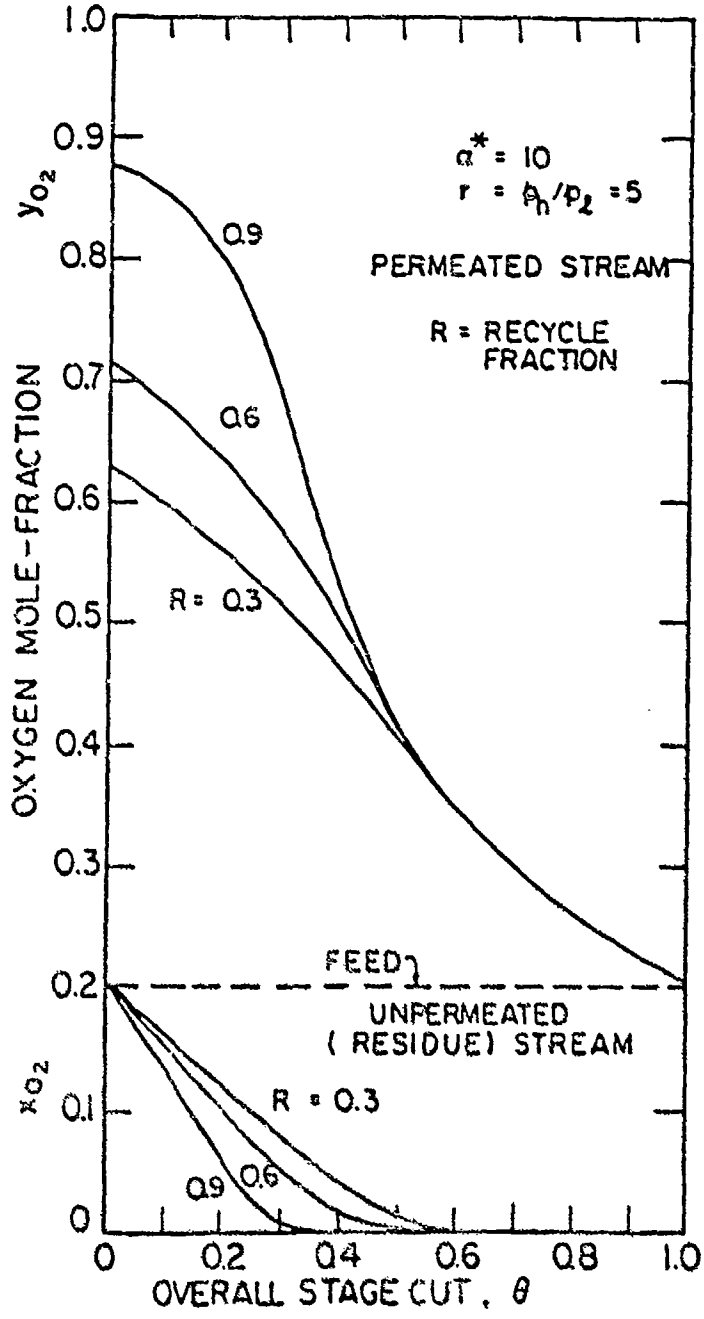

FIGURE 13 Air separation in a continuous membrane column.

permeator. Rather, the concentration of O_2 increases continuously *at constant R* as θ is decreased. The concentration of O_2 also increases *at constant* θ as R is increased, but only at lower values of θ. Therefore, in principle, it should be possible to separate a binary mixture in a CMC to almost any desired extent by operating this device at a sufficiently high R and low θ.

D. Multimembrane Permeators

Onno, Kimura, and their coworkers (29–33) have made the ingenious suggestion that the extent of separation of a binary gas mixture by selective permeation can be substantially enhanced by using two different types of polymer membrane instead of a single type. Each of the two types of membrane is chosen to be selective toward a different component of the mixture to be separated. For example, when separating a mixture of components A and B, one membrane (designated hereafter as membrane A) must be more permeable to component A, while the other membrane (designated as membrane B) must be more permeable to component B. A diagram of a permeator enclosing two different types of membrane simultaneously is shown in Figure 14. As is seen from the figure, the high-pressure feed is separated into *three* product streams:

a) A permeated (low-pressure) stream $P_2(A)$ produced by membrane A and enriched in component A;
b) A permeated (low-pressure) stream $P_2(B)$ produced by membrane B and enriched in component B;
c) An unpermeated (high-pressure) stream P_1, which can be either enriched or depleted in component A.

The extent of separation achievable in a two-membrane permeator and the required membrane areas depend on the same factors as listed previously for single-membrane permeators; however, one has to consider two independent stage cuts θ_A and θ_B, one for each membrane, and (if necessary) two different pressures for the two permeated streams.

Mathematical models describing the separation of binary and multicomponent mixtures in two-membrane permeators have been developed recently for a variety of operating conditions (34–36). Typical results are presented in Figure 15 for a hypothetical mixture of components A and B, and for two hypothetical membranes A and B with reversed selectivities for the components of the mixture [$\alpha_A^*(A/B) = 10$ and $\alpha_B^*(A/B) = 0.1$, where the subscripts designate the membrane type].

Figure 15 shows the concentration of component A in the three product streams as a function of the stage cuts θ_A and θ_B. It is seen that, for any

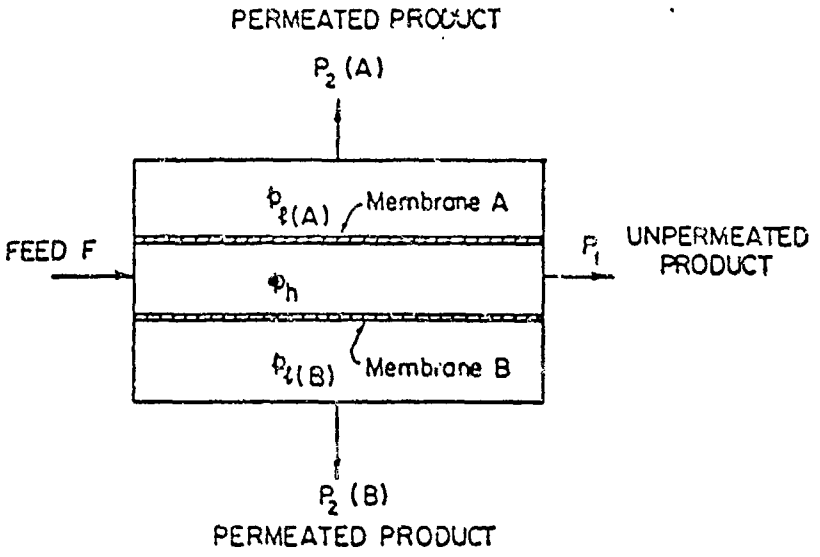

MEMBRANE A IS MORE PERMEABLE TO COMPONENT A

MEMBRANE B IS MORE PERMEABLE TO COMPONENT B

STAGE CUTS : $\theta_A = P_{2(A)}/F$; $\theta_B = P_{2(B)}/F$

FIGURE 14 Diagram of permeator with two different types of membrane.

given value of θ_A, the concentration of component A increases as θ_B is increased, particularly in the permeate from membrane A. This behavior is due to the fact that, as θ_B increases, more component B permeates through membrane B. Therefore, the unpermeated (high-pressure) stream is enriched in component A; the permeate from membrane A is then also enriched in that component. Figure 15 also shows that a much higher separation can be achieved in a two-membrane permeator than in

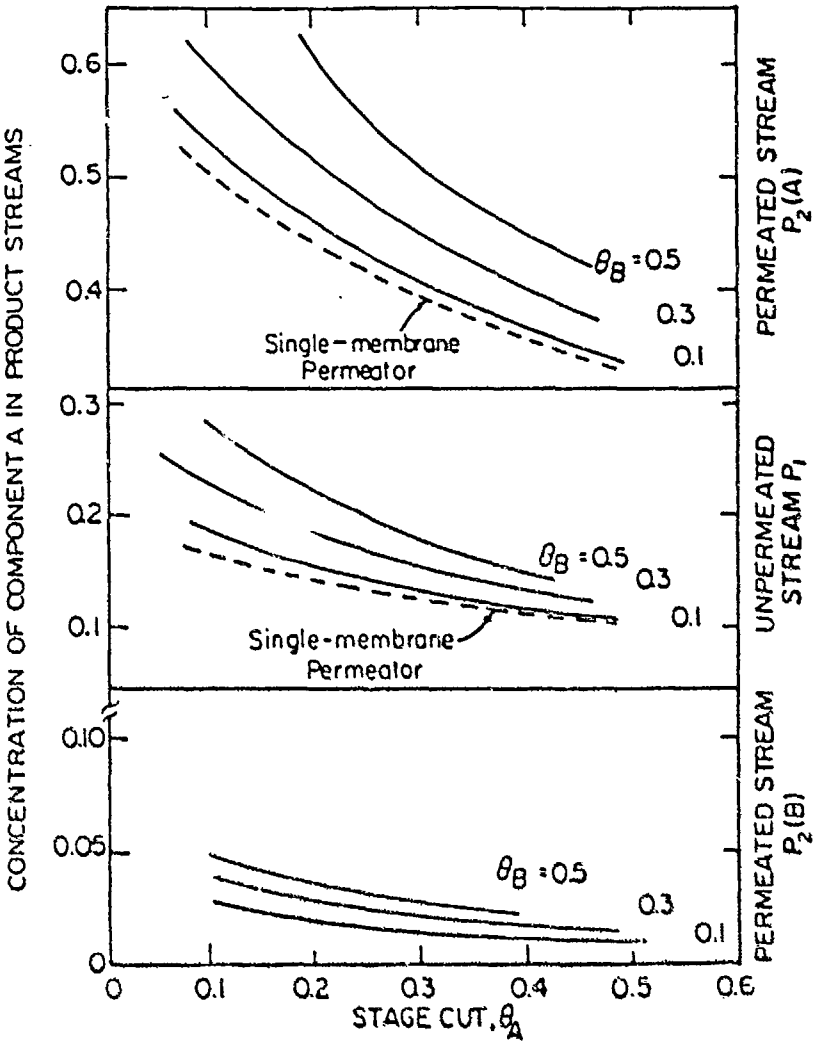

FIGURE 15 Effect of "stage cuts" on compositions of product streams from a two-membrane permeator. $\alpha_A^* = 10$; $\alpha_B^* = 0.1$; $r_A (\equiv p_A/p_{f(A)}) = 5$; $r_B (\equiv p_A/p_{f(B)}) = 5$ "Perfect mixing" conditions. Concentration of component A in feed: 21 mole-%.

a single-membrane permeator provided with membrane A, provided that $\sigma_B^*(A/B)$, θ_B, and r_B are sufficiently large (r_B is the ratio of pressures $p_h/p_{\ell(B)}$ on the two sides of membrane B).

Two-membrane and single-membrane permeators also differ in other respects. For example, the most efficient mode of operating a two-membrane permeator, i.e. the mode yielding the highest degree of gas separation and requiring the smallest membrane area, could be either under countercurrent flow or "perfect mixing" conditions, depending on the relative values of the stage cuts θ_A and θ_B (see Figure 16). By contrast, countercurrent flow is always the most efficient mode of operating a single-membrane permeator.

E. Permeators with Purge Streams

A concept which is not new, but which seems to have received relatively little attention, is the use of a "purge" or "sweep" gas on the permeate (low-pressure) side of a permeator. This procedure would decrease the partial pressures of the permeate components, and thus increase the rates of permeation of these components through the membrane. A theoretical analysis (23) has shown that, with the proper amount of purging, the membrane area requirement would be significantly reduced with only insignificant dilution of the permeated product. If the permeator is operated countercurrently, a small fraction of the feed stream could be used as purge gas. The best results are obtained by purging with an easily condensable gas: not only is the membrane area then reduced, but the dilution of the permeated product can be prevented by condensing out the purge gas (23).

V. MEMBRANE SELECTION

A. Synthetic Polymer Membranes

The "heart" of any permeation process is the membrane that will perform the desired separation. If the permeation process is to compete with conventional separation techniques from an economic standpoint, the membrane must exhibit the following properties:

1. A high permeability towards a specific component (or components) to be separated from a gas mixture.
2. A high selectivity for this component, that is, a high permeability relative to the other components of the mixture.
3. Chemical inertness and physical stability.

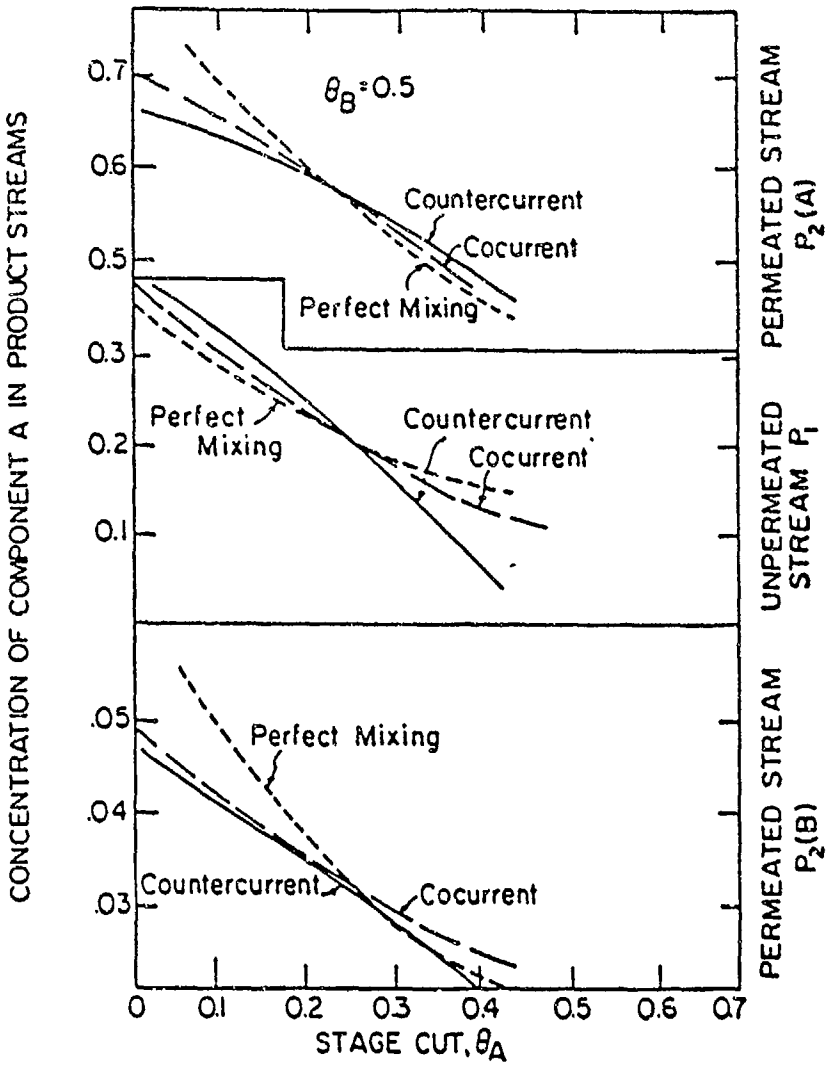

FIGURE 16 Effect of flow pattern on compositions of product streams from a two-membrane permeator. $\alpha_A^* = 10$; $\alpha_B^* = 0.1$; $r_A(\equiv p_N/p_{I(A)}) = 5$; $r_B(\equiv p_A/p_{I(B)}) = 5$ "Perfect mixing" conditions. Concentration of component A in feed: 21 mole-%.

4. Continuity, that is, absence of pinholes or other mechanical defects.

A high permeability and selectivity are required in order to minimize capital investment and power costs (the selectivity must be sufficiently high to yield, at least, the desired product compositions at a practical value of the pressure ratio r). The necessity for chemical inertness and physical stability is self-explanatory. Membrane continuity is required in order to obtain the maximum selectivity characteristic of the membrane. The presence of pores or pinholes in the membrane will greatly reduce, and even destroy, the selectivity for the desired components, because of Knudsen flow or other types of gas transport through such imperfections.

Unfortunately, nature is unkind to the designer of membrane separation processes because available polymer membranes that are highly gas-selective exhibit a low *intrinsic* permeability, and vice versa. This is illustrated in Table II, which lists permeability coefficients and ideal separation factors for He, N_2, and CH_4 in a number of membranes. An examination of this table shows that the membranes which are highly permeable are most often in the rubbery polymer state at the indicated temperature, whereas the membranes which are highly selective are in the glassy state.

The problem of producing a gas separation membrane that exhibits *both* a high permeability and a high gas-selectivity was solved in the early

TABLE II

Permeability coefficients and separation factors for He, N_2, and CH_4 in different polymers

Polymer	Temperature, T(°C)	Permeability coefficient, $\bar{p}$(He) × 10^{10}*	Ideal separation factor, α^*(A/B)	
			He/N_2	He/CH_4
Poly(1-trimethylsilyl-1-propyne)	25	4100	1.95	0.98
Silicone rubber	30	230	1.5	0.39
Nitrile silicone rubber	30	79	3.8	0.79
Ethyl cellulose (ethocel 610)	25	35.6	10.8	4.8
Polycarbonate	30	67	15	19
Teflon FEP	30	62	25	44
Polystyrene	30	35	16	15
Viton A	30	17	55	110
Polyamide (Nylon 6)	25	2.93	98.8	—
Poly(ethylene terephthalate) (Mylar)	25	1.00	167	167
Polyvinyl fluoride	25	0.97	231	171
Poly(vinylidene chloride) (Aran)	25	0.066	366	263

* $\bar{p}$(He) is in units of cm^3 (STP)·cm/(s·cm^2·cm Hg)

1960's by Loeb and Sourirajan (3). These investigators developed the now well-known "phase inversion" method for the formation of high-flux, asymmetric membranes (12, 37–41). While orginally intended for the desalting of saline water by the reverse osmosis process, asymmetric membranes are now used also for gas separations.

A cross-section through an asymmetric membrane is shown in Figure 17(a). The membrane consists of a microporous layer (100–200 μm-thick), one side of which is covered with a very thin (0.1–1.0 μm), *nonporous* "skin" or surface layer. The separation of gas mixtures through an asymmetric membrane occurs in its skin, while the microporous substrate provides the membrane with mechanical strength. The rate of gas permeation through such a membrane will be very high because it is inversely proportional to the *effective* membrane thickness, which is that of the nonporous skin. The gas-selectivity of an asymmetric membrane can also be high if, as mentioned above, the membrane is in the glassy state. Asymmetric membranes were first prepared from cellulose acetate, but can now be made from a variety of polymeric materials.

It should be noted that asymmetric membranes may contain solvent and water from the casting and coagulation stages in their preparation, and therefore must be carefully dried before being used as gas separation barriers. Otherwise, the slow removal of solvent and water from the membranes by the permeating gases will cause a continuous increase in the thickness of their dense skin, due to the gradual collapse of the microporous substrate. This will result, in turn, in a corresponding decrease in the membrane permeability. Several methods are now available for drying asymmetric membranes without increasing their skin thickness (42–44).

Another method of preparing an asymmetric membrane is to *laminate* an ultrathin (0.05–0.1 μm), nonporous film to a much thicker (100–200 μm) microporous backing, or support layer, as is shown in Figure 17b. The ultrathin film and backing of this composite membrane, which is sometimes called a "thin-film laminate", have the same functions as the skin and microporous substrate, respectively, of an asymmetric membrane of the type described above. However, the ultrathin film and its backing are made of different materials, whereas the skin of an asymmetric membrane is an integral part of its substrate. As a result, the properties and performance of a thin-film laminate can be better controlled, in principle, than those of a "skinned" membrane. Unfortunately, the preparation of ultrathin films is a delicate operation which cannot be readily automated or scaled up (12, 40–41, 45–49).

A third method of preparing an asymmetric membrane is by *coating* a thin nonporous film directly on the surface of a suitable microporous

backing. This coated-film composite differs from a thin-film laminate in that the coating penetrates into the pores of its backing material, as is illustrated in Figure 17c. Consequently, the coating is strongly bonded to its backing. A variety of techniques of preparing coated-film composites have been described in the literature, cf. refs. (12) and (39–41). An important advantage of coated-film composites is that these can be prepared so that the separation of gas mixtures permeating through such membranes occurs either in the coated film or in its backing (e.g. if the backing is itself a "skinned" membrane).

Some asymmetric membranes, such as the "skinned" membranes and the coated-film composites, can be produced in the form of *hollow fibers*

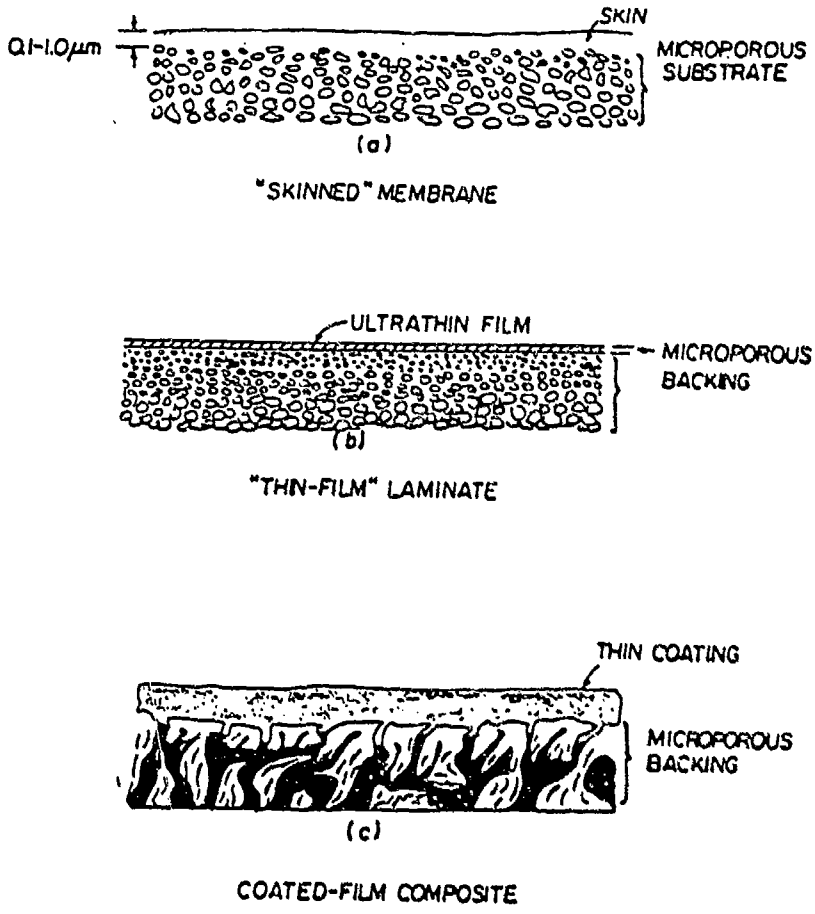

FIGURE 17 Asymmetric membranes.

with inner diameters varying from a few tenths to a few hundreds μm. A cross-section of a "skinned" asymmetric hollow fiber is presented in Figure 18; the nonporous skin is shown on the outer surface of the hollow fiber, but could as well be formed on its inner surface. Hollow-fiber permeators (see Figure 3) are the most efficient membrane separation devices because they can pack much larger membrane areas per unit volume ($>10{,}000\,m^2/m^3$) than permeators provided with membranes in sheet or tubular form ($\leq 1{,}000\,m^2/m^3$). Hollow-fiber permeators do not require membrane supports and separators, as do permeators utilizing sheet membranes (plate-and-frame and spiral wound permeators). Moreover, hollow fibers can withstand pressure differences as high as 100 atm. across their walls if they are sufficiently rigid, e.g. if in the glassy state, and if the wall thickness is adequate [O.D./I.D. ≈ 2, ref. (3)].

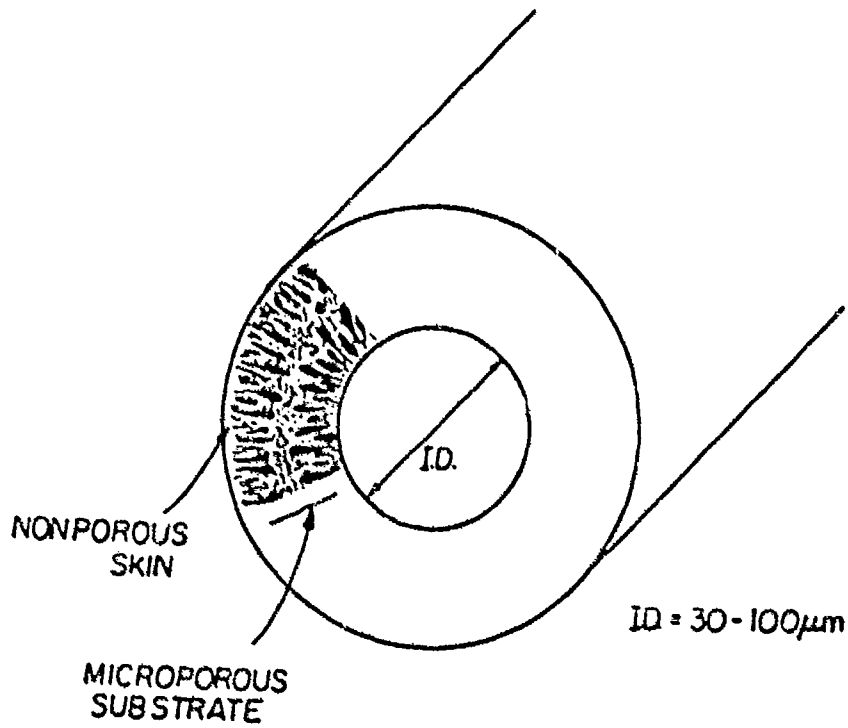

FIGURE 18 Asymmetric hollow fiber

The composite hollow fibers used so successfully by Monsanto Company in its PRISM permeators for the separation of H_2 from various industrial gas mixtures are "skinned" asymmetric hollow fibers of polysulfone coated with a thin film of silicone rubber (~1 μm-thick). The polysulfone skin, which is about 0.1 μm-thick, is the separative element, while the only function of the silicone rubber coating is to plug whatever micropores or discontinuities may be present in the skin (12, 50–52). Polysulfone has a much higher gas-selectivity than silicone rubber. A number of other composite hollow fibers of this type have been studied, for example, polysulfone (1) — polyethylene (2), poly(acrylonitrile (1) — silicone rubber (2), and poly(acrylonitrile)-polyethylene (2), where (1) designates the "skinned" hollow fiber and (2) designates the coating (50–52). No coating is required in cases where the skin is nonporous.

B. Facilitated-Transport Membranes

The rate of permeation of a gas through a membrane can be greatly enhanced by means of an auxilliary mode of transport known as "facilitated" or "carrier-mediated" transport. This mode may be induced in some cases by a reversible chemical reaction between the penetrant gas and a mobile carrier, which is incorporated in the membrane and shuttles between the membrane interfaces (11). Facilitated-transport of a component of a permeating mixture can substantially increase the selectivity of the membrane toward that component.

Conside the permeation of a mixture of components A and B through the facilitated-transport membrane shown diagramatically in Figure 19. such a membrane consists of a microporous support which is impregnated with a non-volatile liquid; the liquid is strongly held in the pores of the membrane by capillary forces. A mobile carrier C which can react reversibly with, say, component A is dissolved in the liquid. The reversible reaction is

$$A + C \rightleftharpoons AC,$$

where AC is a complex.

If a pressure (and concentration) gradient of A and B is imposed across the membrane, from left to right, the *forward* reaction will take place at the left interface of the membrane to form AC. A concentration gradient of AC is therefore established in the same direction as that of A. The complex AC then diffuses to the right interface, where the *reverse* reaction takes place to reform A and C. Component A is released from

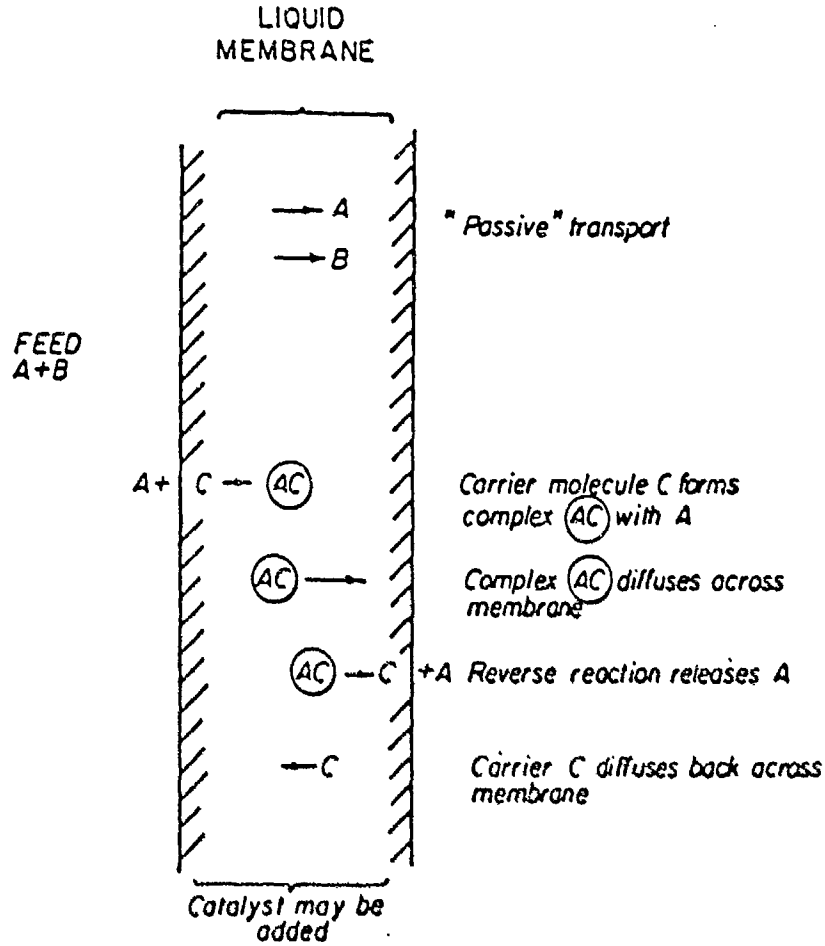

FIGURE 19 Facilitated transport membrane.

solution at the right interface of the membrane. Carrier C, being a nonvolatile molecular or ionic species, diffuses back to the left interface, where it reacts again with A. Thus, C shuttles back and forth between the two membrane interfaces and facilitates the transport of A. The net transport of C is equal to that of AC but in opposite direction.

The selectivity of the membrane is greatly enhanced by the above process, because component A permeates through the membrane both by facilitated transport and by "passive" transport (Fickian diffusion without

chemical reaction), whereas component B permeates only by passive transport. The reaction between A and C can be accelerated by addition of a suitable catalyst.

Facilitated transport in synthetic membranes, which mimics a similar process in biological membranes, was studied by Ward (53–57) and by other investigators [see (12) for pertinent references]. It is beyond the scope of this paper to discuss the mechanism of facilitated transport, which has been reviewed elsewhere (58, 59), or the various modifications of this process (12). Facilitated-transport membranes have been developed for O_2, CO_2, CO, H_2S, NO, and olefins, but all suffer from a variety of limitations (12), and therefore have not found as yet any practical applications. The facilitated transport of O_2 is particularly important in air separation, because solid polymer membranes have relatively low separation factors [$^*(O_2/N_2) \leq 6$]. A facilitated-transport membrane for O_2 with $\alpha^*(O_2/N_2 = 30$, yielding over 80% O_2, has been developed recently (60). The practical lifetime of this membrane was limited to a few weeks at ambient temperature, or to 3 months at -10°C., because the carrier (a metal-organic complex) oxidized irreversibly and lost gradually its chemical activity.

VI. FUTURE DEVELOPMENTS

The prediction of future developments in membrane separation processes is fraught with danger, because these developments will depend as much on uncertain economic factors, such as the cost of energy, as on technological factors. For example, who would have predicted in 1972 that the cost of oil would quadruple in the interval of one year?

Membrane separation technology has made remarkable progress in the last two decades. The principles of membrane process and equipment design are now well understood, and have been tested on a large scale under field conditions. New membrane processes for the separation of gases will undoubtedly emerge in the coming years. However, the rate of progress of the last 20 years will be sustained only if more highly gas-selective and permeable membranes than available at present can be synthesized. This will require that significant progress be made, in turn, in our understanding of the relationships between the chemical structure of polymers and their gas permeability.

The prior discussion should have made it clear that the selection of a polymer membrane for the separation of a specific gas mixture is based at present on rather primitive considerations. Usually, a process simulation

coupled with a preliminary economic analysis first establishes what selectivity and permeability the membrane must exhibit in order to ensure the economic viability of the process. A search is then made in the literature, or in whatever data base is available, for a membrane with the desired properties. If such a membrane indeed exists it is likely to be in the glassy polymer state because, as mentioned earlier, glassy polymers are more gas-selective than rubbery ones (6, 7). However, glassy polymers also exhibit, in general, a low *intrinsic* permeability (i.e. low values of the permeability coefficient $\bar{P}$). Therefore, in order to obtain the desired rate of gas permeation, the selected membrane will have to be used in symmetric or composite form.

It is more likely, however, that no membrane endowed with all the required properties will be found to exist. The desired membrane must then be synthesized by the polymer chemist. The relationships between the chemical structure of polymers and their selectivity and permeability to different gases is not well understood. Therefore, the structure of new membranes with specified permeability characteristics can be found at present only based on some qualitative observations (5, 12, 61), on some semiempirical but useful solubility and diffusivity correlations [e.g. ref. (62)], and on considerable trial-and-error.

Finally, it has been shown earlier that the gas-selectivity of polymer membranes varies inversely, in general, with their intrinsic permeability. Can polymers that exhibit *both* a high selectivity and a high permeability be synthesized? Table III suggests that this might be possible. For example, Japanese investigators (63) have recently developed an acetylenic polymer, poly[1-(trymethylsilyl)-1-propyne)] (PMSP), that exhibits a gas permeability (toward O_2, N_2, CO_2, CH_4, and He) that is about an order of magnitude higher than that of silicone rubber (PDMS). It was previously thought that PDMS was the most gas-permeable polymer because of its large free volume and the flexibility of its Si−O bond. By contrast, PMSP is a fairly rigid polymer because its backbone contains alternating double bonds. It is particularly interesting that the O_2/N_2 selectivity of PMSP is about equal to that of PDMS, while the CO_2/CH_4 selectivity is higher.

Table III also shows that the glassy polymers poly(methylpentene) and poly(oxydimethyl phenylene) exhibit a higher O_2 permeability at 25°C than rubbery polyethylene and butyl rubber, and as high a permeability as that of Buna S. At the same time, the O_2/N_2 selectivity of the two glassy polymers is higher than that of the three rubbery polymers. Clearly, much remains to be learned in this field.

Significant efforts are being made at present in a number of academic and industrial laboratories to advance the materials science of gas

TABLE III

Selected gas permeabilities and separation factors of rubbery and glassy polymers

Polymer	Permeability coefficients, $\bar{p} \times 10^{10}$ cm³(STP)cm/(s·cm²·cm Hg)				Ideal separation factor, $\alpha^*(A/B)$	
	O_2	N_2	CO_2	CH_4	O_2/N_2	CO_2/CH_4
Rubbery Polymers						
Poly(1-trimethylsilyl-1-propyne) *	4200	2100	18000	4200	2.0	4.3
Poly(dimethylsiloxane)	500	238	2700	800	2.1	3.4
Natural rubber	24	8.1	131	30	3.0	4.4
Buna-S	17.1	6.32	124	21	2.7	5.9
Polyethylene($\rho = 0.914$)	2.9	0.97	12.6	2.9	3.0	4.3
Butyl rubber	1.3	0.33	5.18	0.78	3.9	6.6
Glassy Polymers						
Poly(methylpentene)	18.9	4.5	—	—	4.1	—
Poly(oxydimethyl phenylene)	15.8	3.81	75.7	—	4.1	—
Polystyrene	2.47*	2.55*	23.3*	2.73*	2.9	8.5*
Poly(bis a carbonate) (Lexan)	1.40	0.300	10*	0.5*	4.7	20*
Polysulfone**	—	0.19	6.4	0.23	—	28**
Poly(vinyl fluoride)	0.029	0.0042	—	—	4.8	—

$\alpha^*(A/B) = \bar{p}_A/\bar{p}_B$; temperature = 25°C; *35°C, **35°C.

*Recent studies show that poly(1-trimethylsilyl-1-propyne) is a glassy polymer.

separation membranes. These efforts should reself in important new developments in membrane technology for gas separations.

ADDENDUM: A detailed study of recycle permeators has recently been reported by McCandles (63).

REFERENCES

1. T. Graham, Phil. Mag., *32*, 401 (1866)
2. G. Parkinson, Chemical Engineering, April 16 (1984), p. 14
3. S. Loeb and S. Sourirajan, "Sea Water Demineralization by Means of a Semipermeable Membrane," University of California (Los Angeles), Dept. Eng. Repts., No. 60–60 (1961).
4. C.E. Rogers, "Solubility and Diffusivity", Chapt. 6 in "Physics and Chemistry of the Organic Solid State", D. Fox, M.M. Labes, and A. Weissberger, Eds., Interscience Publishers, New York, 1965, pp. 510–635.
5. S.A. Stern, "Gas Permeation Processes", Chapt. XIII in "Industrial Processing with Membranes", R.E. Lacey and S. Loeb, Eds., Wiley-Interscience, New York, 1972, pp. 279–339.
6. S.A. Stern and H.L. Frisch, Ann. Rev. Mater. Sci., *11*, 523 (1981).
7. H.L. Frisch and S.A. Stern, "Diffusion of Small Molecules in Polymers", CRC Crit. Rev. in Solid State and Mat. Sci., *11*, No. 2, 123–187 (1983), CRC Press, Boca Raton, FL.
8. J. Crank, "The Mathematics of Diffusion", 2nd Ed., Clarendon Press, Oxford, 1975
9. W. Jost, "Diffusion in Solids, Liquids, Gases", Academic Press, New York, 1952
10. S.-T. Hwang and K. Kammermeyer, "Membranes in Separations", Wiley-Interscience, New York, 1975
11. S.A. Stern, "The Separation of Gases by Selective Permeation" Chapt. 9 in "Membrane Separation Processes", P. Meares, Ed., Elsevier Scientific, New York, 1976, pp. 296–326
12. S.L. Matson, J. Lopez, and J.A. Quinn, Chem. Eng. Sci., *38*, 503 (1983)
13. S. Weller and W.A. Steiner, J. Appl. Phys., *21*, 279 (1950)
14. S. Weller and W.A. Steiner, Chem. Eng. Progr., *46*, 585 (1950)
15. R.W. Naylor and P.O. Backer, AIChE J., *1*, 95 (1955)
16. M.E. Brewer and K. Kammermeyer, Separation Sci., *2*, 319 (1967)
17. S.A. Stern and W.P. Walawender, Separation Sci., *4*, 129 (1969)
18. W.P. Walawender and S.A. Stern, Separation Sci., *7*, 553 (1972)
19. C.T. Blaisdell and K. Kammermeyer, Chem. Eng. Sci., *28*, 1339 (1973)
20. C.Y. Pan and H.W. Habgood, Ind. Eng. Chem. Fundam., *13*, 323 (1974)
21. C.Y. Pan and H.W. Habgood, Can. J. Chem. Eng., *56*, 197 (1978); ibid., *56*, 210 (1978)
22. S.A. Stern and S.-C. Wang, J. Membrane Sci., *4*, 141 (1978)
23. S.A. Stern and F.J. Onorato, and C. Libove, AIChE J., *23*, 567 (1977)
24. S.A. Stern and S.M. Leone, AIChE J., *26*, 881 (1980)
25. S.A. Stern and S.-C. Wang, AIChE J., *26*, 891 (1980)
26. S.A. Stern, J.E. Perrin, and E.J. Naimon, J. Membrane Sci., *20*, 25 (1984)
27. W.C. Pfefferle, U.S. Patent No. 3,144,313, August 11, 1964
28. S.-T. Hwang and J.M. Thorman, AIChE J., *26*, 558 (1980)
29. S. Kimura, T. Nimura, T. Miyauchi, and M. Ohno, Radiochem. Radioanal. Lett., *13*, 349 (1973)
30. M. Ohno, T. Morisue, O. Ozaki, H. Heki, and T. Miyauchi, Radiochem. Radioanal. Lett., *27*, 299 (1976)
31. M. Ohno, O. Ozaki, and H. Sato, J. Nucl. Sci. Technol. Japan, *14*, 589 (1977)
32. M. Ohno, T. Morisue, O. Ozaki, and T. Miyauchi, J. Nucl. Sci. Technol. Japan, *15*, 376 (1978)

N A V A L S P E C I A L W A R F A R E

DISTRIBUTION LIST

		Copy No.
003	Chief of Naval Operations	
	(OP-353)	1
	(OP- 31)	2
	(OP- 22)	3
	(OP- 21)	4
	Chief of Naval Research (Office of Naval Technology)	
	800 North Quincy Street, Arlington, VA	5
	22217-5000	6
	(ONT- 23, Dr. A.J. Faulstich)	7
	(ONT-235 Dr. W. Ching)	
	(ONT-23D CAPT. R.S. Fitch)	
427	Commander, Naval Sea Systems Command (NAVSEA-06Z)	8
	Commander, Naval Special Warfare Command (N-8) NAB; Coronado, CA	9
	Commander, Naval Special Warfare, Group 1 NAB; Coronado, CA	10
	Commander, Naval Special Warfare, Group 2 Little Creek, VA	11
310	Commander, Submarine Development Squadron TWELVE	12
600	Commander, Surface Warfare Development Group	13
	Commander, Naval Coastal Systems Center (Library)	14
210	Commander, Naval Surface Weapons Center, White Oak (Library)	15
277	Officer in Charge, Naval Underwater Systems Center New London Laboratory, (Library)	16
278	Commanding Officer, Naval Underwater Systems Center Newport Laboratory (Library)	17
265	Commanding Officer, Naval Oceans Systems Center, San Diego (Library)	18

621	Commanding Officer, Naval Oceans Research and Development Activity Bay St. Louis (Library)	19
267	President, Naval War College (Library)	20
222	Superintendent, Naval Postgraduate School (Library)	21
075	Director, Defense Technical Information Center	22-23